(NASA-CR-158023) COMPOSITE STRUCTURAL MATERIALS Semi-annual Progress Report, April 1978 - September 1978 (Rensselaer Polytechnic Inst., Troy, N. Y.) 84 p HC A05/MF A01 CSCL 11D G3/24

N79-14157

Unclas 41803

COMPOSITE STRUCTURAL PROGRAM

RENSSELAER POLYTECHNIC INSTITUTE TROY, N.Y. 12181

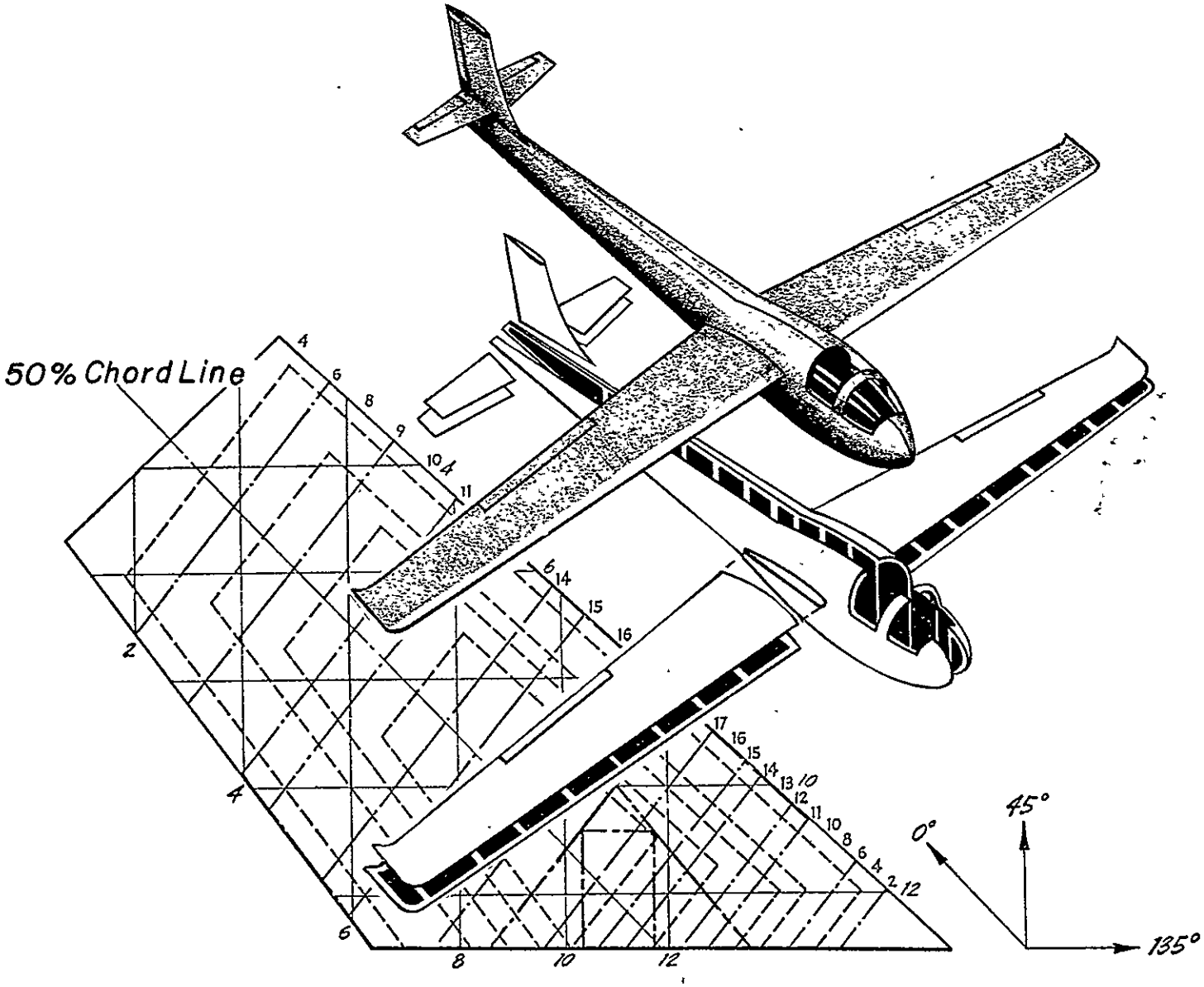

SKIN DESIGN

REPRODUCED BY
NATIONAL TECHNICAL INFORMATION SERVICE
U.S. DEPARTMENT OF COMMERCE
SPRINGFIELD, VA. 22161

SPONSORED BY
NASA/AFOSR

Semi-Annual Progress Report

April 1978 - September 1978

COMPOSITE STRUCTURAL MATERIALS

Air Force Office of Scientific Research
and
National Aeronautics and Space Administration
Grant No. NGL 33-018-003

Co-Principal Investigators:

George S. Ansell
Dean, School of Engineering

and

Stephen E. Wiberley
Dean, Graduate School and Vice Provost

Rensselaer Polytechnic Institute
Troy, New York 12180

NASA Technical Officer:

Michael J. Salkind
Materials and Structures Division
NASA Headquarters

35th Semi-Annual Progress Report December 1978

CONTENTS

	Page
INTRODUCTION	1
PART I. CAPCOMP (Composite Aircraft Program Component), N. J. Hoff and Y. Hirano	10
PART II. CAPGLIDE (Composite Aircraft Program Glider), E. J. Brunelle, R. J. Diefendorf, H. J. Hagerup, G. Helwig, N. J. Hoff	18
1. Pilot Accommodations and Control Fixtures - 5 Students	19
2. Aerodynamics, Stability and Control - 6 Students	20
3. Design Modification - Faculty and Staff	21
4. Aeroelastic Studies	35
A. Introduction and Overview	35
B. Static Stability and Control Problems; Rate of Sink and Range Problems	37
C. Flutter Involving Complete Aircraft Motion	39
D. Summary	51
5. Fabrication and Testing	51
A. Introduction	51
B. Materials	52
C. Molds	56
D. Fabrication - Wing	59
E. The CFRP Box Section Spar	60
PART III. COMPAD (Computer Aided Design), L. J. Feeser	64
PART IV. SUPPORTING RESEARCH	67
Resin Matrix Characterization, S. S. Sternstein	68
Fatigue in Composite Structures, K. Krempl	71
Ultrasonic Non-Destructive Testing of Composite Structures, H. F. Tiersten and P. K. Das	73
Metal Matrix Composites, N. S. Stoloff	76
PART V. PERSONNEL, AUTHOR INDEX	79
PERSONNEL	80
AUTHOR INDEX	83

INTRODUCTION

Technological demand for improved performance in materials has always existed. The recent interest in composite materials has been generated by the ability to use brittle materials with high modulus, high strength, but low density in composites which fail in a non-catastrophic manner. These fiber reinforced composite materials offer improved performance and potentially lower costs for aerospace hardware.

However, the application of composite materials to sophisticated aerospace structures requires a strong technology base. NASA and AFOSR have realized that to fully exploit composites the technology base must be improved, both in terms of expanding fundamental knowledge and the means by which it can be successfully applied in design and manufacture and also in the body of engineers and scientists competent in these areas. As part of their approach to accomplishing this, they have funded the current composites program at Rensselaer. The purpose of the RPI composites program is to develop advanced technology in the areas of physical properties, structural concepts and analysis, manufacturing, reliability and life prediction. Concommitant goals are to educate engineers to design and use composite materials as normal or conventional materials. A multifaceted program has been instituted to achieve these objectives.

The major elements of the program are:

1. CAPCOMP (Composite Aircraft Program Component). CAPCOMP is primarily a graduate level project being conducted in parallel with a composite structures program sponsored by NASA and performed by a private, aerospace manufacturing contractor, the Boeing Commercial Airplane Company. The main spar/rib region on the Boeing 727 elevator, near its actuator attachment point, has been tentatively selected as the component for study in CAPCOMP. The magnitude of the project - studying, designing, fabricating and testing the most highly stressed region on the elevator - is both consistent with Rensselaer's capabilities, and a significant challenge. The selection of a portion of a full scale flight hardware structure assures relevance to this project's direction. Visits to Boeing are planned for early in the Fall of 1978 on the part of Professor Hoff and several of his students, and the first serious design work will begin shortly thereafter. Some supportive analysis for CAPCOMP is described briefly in Part I.

2. CAPGLIDE (Composite Aircraft Program Glider). This undergraduate demonstration project is to design, fabricate and test an ultralight glider using composite structures. A flight vehicle was selected to maximize student interest and to provide the students with a broad-based engineering experience. The progress on the CAPGLIDE project to date has been very satisfactory. Four professors

and approximately 35 students were actively engaged in the project during the beginning of this period; that is, prior to the end of the Spring semester. Our first "NASA/AFOSR Visiting Associate", Dr. Gunter Helwig, joined the project at that time, bringing a wealth of experience as Akaflieg advisor at the Technical University of Darmstadt. With Dr. Helwig here, faculty and staff made a detailed review of the CAPGLIDE status over the summer. The description of the work performed under CAPGLIDE is given in Part II.

3. COMPAD (Computer Aided Design). A major thrust of the composites program is to develop effective and efficient tools for the analysis and design of composite structures. Rensselaer and NASA Langley have jointly implemented the use of the SPAR code on minicomputers. In addition, Rensselaer has embarked on converting an interactive graphics display capability for SPAR use. More complete details are reported in Part III.

4. Composites Fabrication and Test Facility. Structural design engineers, educated only by course work and design projects limited to paper, often fail to sense or appreciate problems involved in fabrication. The actual fabrication and testing of composite structural components provides this training and the final validation for the designs in our CAP projects. RPI's Composites Fabrication and Test Facility is located in the laboratory and high bay areas of the Jonsson Engineering Center. Equipment is

available for compression molding parts as large as 19" x 19" and vacuum bagging parts up to 4' x 8'. Ultimately, panels as large as 5' x 20' will be made by vacuum bagging. A pressure vessel for small parts and spars has been designed and was built during the last report period. Prices for various pieces of specific test equipment for both materials and components evaluated during the last period were obtained, and a letter requesting NASA/AFOSR approval to order them was submitted at the end of the period. More complete details are reported in Part II under CAPGLIDE.

5. Research Programs. The criteria for selection of research projects to be conducted under this program are (a) that they must anticipate critical problem areas which may occur in the CAP or NASA/AFOSR programs or (b) that solutions to existing problems are not yet satisfactorily in hand. During the last period five programs were funded; a total of nine programs were budgeted for the current period. Results from the ongoing projects are reported in Part IV.

6. Curriculum Revisions. The goal of educating engineers to think of composites as normal or conventional materials has required changes in curriculum. Since the initiation of this program, almost all Rensselaer engineers take introductory courses which incorporate the concepts of anisotropy and composite materials. In addition, five specialized courses in composites have been offered during the past two years to develop those special skills required of

students involved in the composites program. A "mini course" was presented at RPI by Dr. Stephen W. Tsai of the USAF Materials Laboratory* in August which emphasized the use of programmable hand calculators in designing composite materials. Next year a new course will be introduced on composite design and analysis using central mini and full frame computers. The additions of the SPAR computer code and the growing availability of interactive computer graphics under our COMPAD program element are intended to reach a point where our engineering students will use these facilities as everyday working tools for design, analysis and visualization purposes.

7. Technical Interchange.

a) Student summer employment (SSE): While universities generally consider education in terms of on-campus activities, the composites program is trying to provide hands-on experience through summer placement in industry and government. The SSE program has been one of the most successful parts of the total program. The good performance of our students last summer (1977) and also the considerable effort that the companies made to provide truly challenging jobs was evident in the post-employment reports of the students, those of their industry employers, and the fact that the total number of jobs available for this summer (1978) was

---

* Chief, Mechanics and Surface Interactions Branch of the Non-Metallic Materials Division

several times the number of students. Placement for '77 and '78 is shown in Figure 1. As the program expands, it is anticipated that the number of students involved in the summer employment program will be in the 20 to 30 range. This program expansion should allow for good interaction between industry, government and Rensselaer.

b) Professional interchange: During the latter part of the reporting period, an Industrial Technical Advisory Committee (ITAC) was formed. Its members, shown in Figure 2, are leading figures in composite materials and structures with major, advanced technology companies. The first meeting of the ITAC is currently scheduled to coincide with the 2nd NASA/AFOSR review of the RPI Composites Program. Subsequent meetings will take place as seems appropriate in the course of the program.

As anticipated in the last report, Dr. Christopher LeMaistre has joined the project from his position with the Department of Defense in Australia. Dr. LeMaistre's expertise is in high performance fibers and composites fabrication and his experience includes tours with the Weapons Research Establishment at Salisbury and with the Australian High Commission as Assistant Research and Development Representative in London.

Finally, during this period, Mr. Kiyoshi Kenmochi has joined the project as a Research Associate. His background includes positions with the Composites Engineering section

of Japan's Industrial Products Research Institute and the Materials Division of the Institute of Space and Aeronautical Sciences of the University of Tokyo.

c) Technical meetings: Technical meetings provide important off-campus interchange of technical information. Because of the large number of composites meetings, a central catalog with all upcoming meetings is being maintained. In this way it can be assured that a Rensselaer staff member will participate in important meetings. Meetings attended during the reporting period are shown in Figure 3.

In summary, the NASA/AFOSR Composites Aircraft Program is a multi-faceted program whereby aeronautical, mechanical and materials engineers must interact to achieve its goals. "Hard-nosed" engineering of composite aircraft structures is balanced against research aimed at solving present and future problems. In the following sections, detailed descriptions of the CAPCOMP, CAPGLIDE, COMPAD and research programs are presented.

Figure 1 - STUDENT SUMMER EMPLOYMENT

	1977	1978
NASA Lewis	4	3
NASA Langley	1	0
Naval Air. Dev. Center	0	1
McDonnell Douglas (St. Louis)	5	4

Figure 2 - INDUSTRIAL TECHNICAL ADVISORY COMMITTEE (ITAC)

Dr. Joseph Epel	Director, The Plastics Research and Development Center, The Budd Co., Inc.
Mr. Stanley Harvey	Program Manager, Composites Boeing Commercial Airplane Co.
Mr. Howard Siegel	Manager, Materials and Process Development, McDonnell Aircraft Co.
Mr. Max Waddoups	Design Specialist, Ft. Worth Texas Div. of General Dynamics Corp.

Figure 3 - COMPOSITES-RELATED TECHNICAL MEETINGS ATTENDED

April '78 - September '78

ONR-Electrical Problems in Carbon Fiber Composites
April 10, 11, 1978. MIT, Cambridge, Mass.

AFOSR-Carbon/Carbon Composites Process Science Meeting
April 17, 18, 1978. San Antonio, Texas.

International Meeting on Composites, April 18-20, 1978.
Toronto, Ont.

Conference on the Utilization of Advanced Composites in Commercial Aircraft Wing Structures, April 16, 17, 1978.
NASA Langley Research Center, Hampton, Va.

U.S. National Congress of Applied Mechanics, June 26-30, 1978. Los Angeles, Cal.

ONR-Electrical Problems in Carbon Fiber Composites
July 14-17, 1978. Santa Barbara, Cal.

Fifth Annual Conference on Computer Graphics and Interactive Techniques, August 21-25, 1978. Atlanta, Ga.

Eleventh International Congress of Aeronautical Sciences
September 10-16, 1978. Lisbon, Portugal.

PART I

CAPCOMP (Composite Aircraft Program Component)

CAPCOMP (Composite Aircraft Program Component)

(N. Hoff and Y. Hirano)

CAPCOMP is a program to design flight critical structures to take the maximum advantage of composite materials. By combining the efforts of experienced faculty with bright and well trained but inexperienced graduate students in an environment relatively free of traditional design and manufacturing processes, we hope to devise new and hopefully useful design concepts.

The first such project chosen is the actuator attachment area of a 727 elevator (See Figures 4 and 5). RPI will be carrying forward a 727 elevator structures demonstration program, in parallel with NASA and its aerospace engineering contractor, the Boeing Commercial Airplane Company. This design, fabrication and test effort is to explore new design ideas specifically suited to advanced composite construction for the purpose of minimizing the weight of the structure, but on a scale consistent with the university context and funding level.

Preliminary to undertaking the design of the 727 elevator, an analysis of circular cylindrical shells was undertaken for buckling characteristics. The results of such an analysis for the optimization of laminated circular cylindrical shells for buckling was anticipated as providing useful results for curved shell members in general.

Fig. 4

727 Elevator - Boeing Design

— basic aluminum structure
— parts replaced by composites
parts kept in aluminum

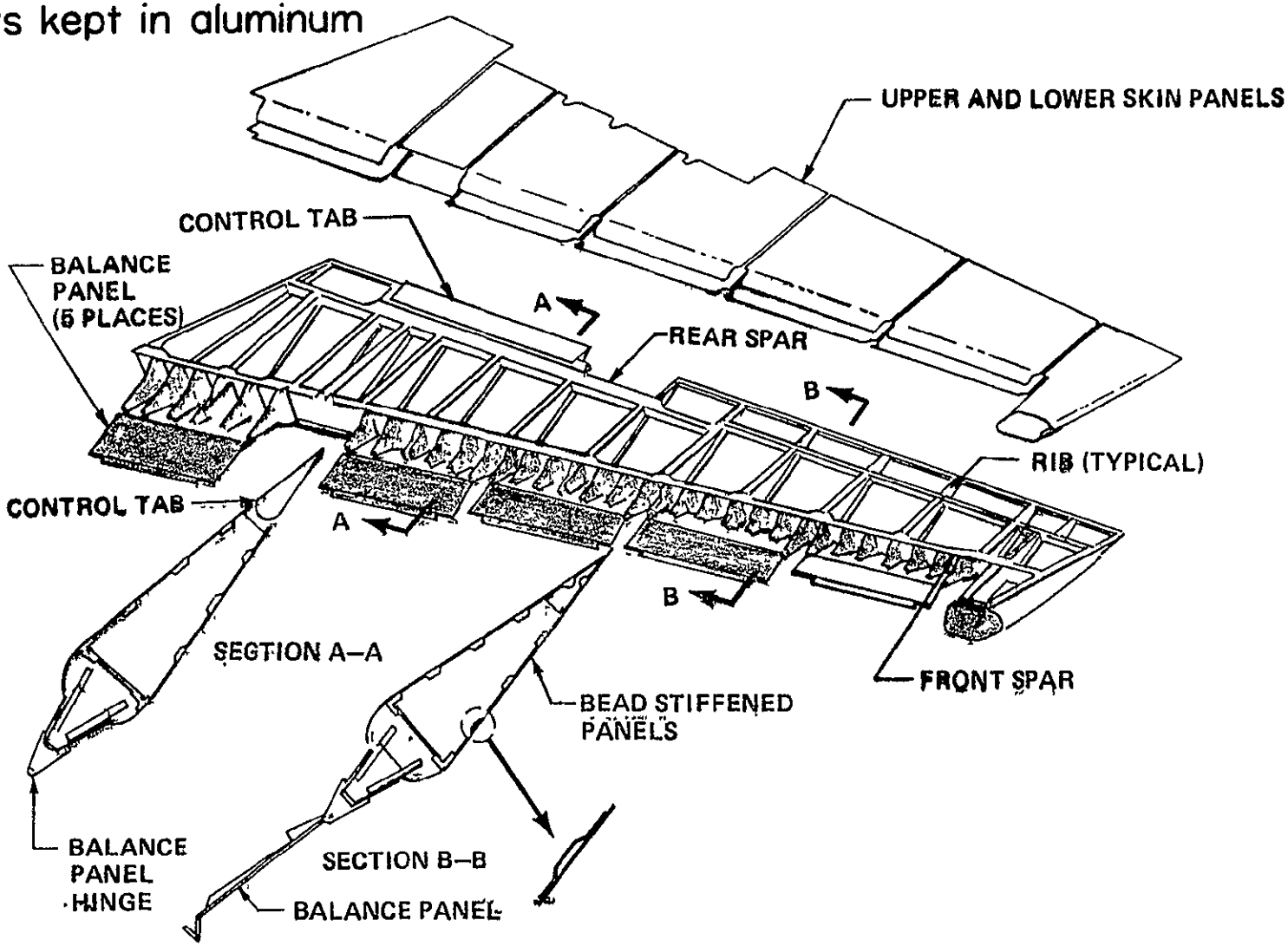

Fig.5

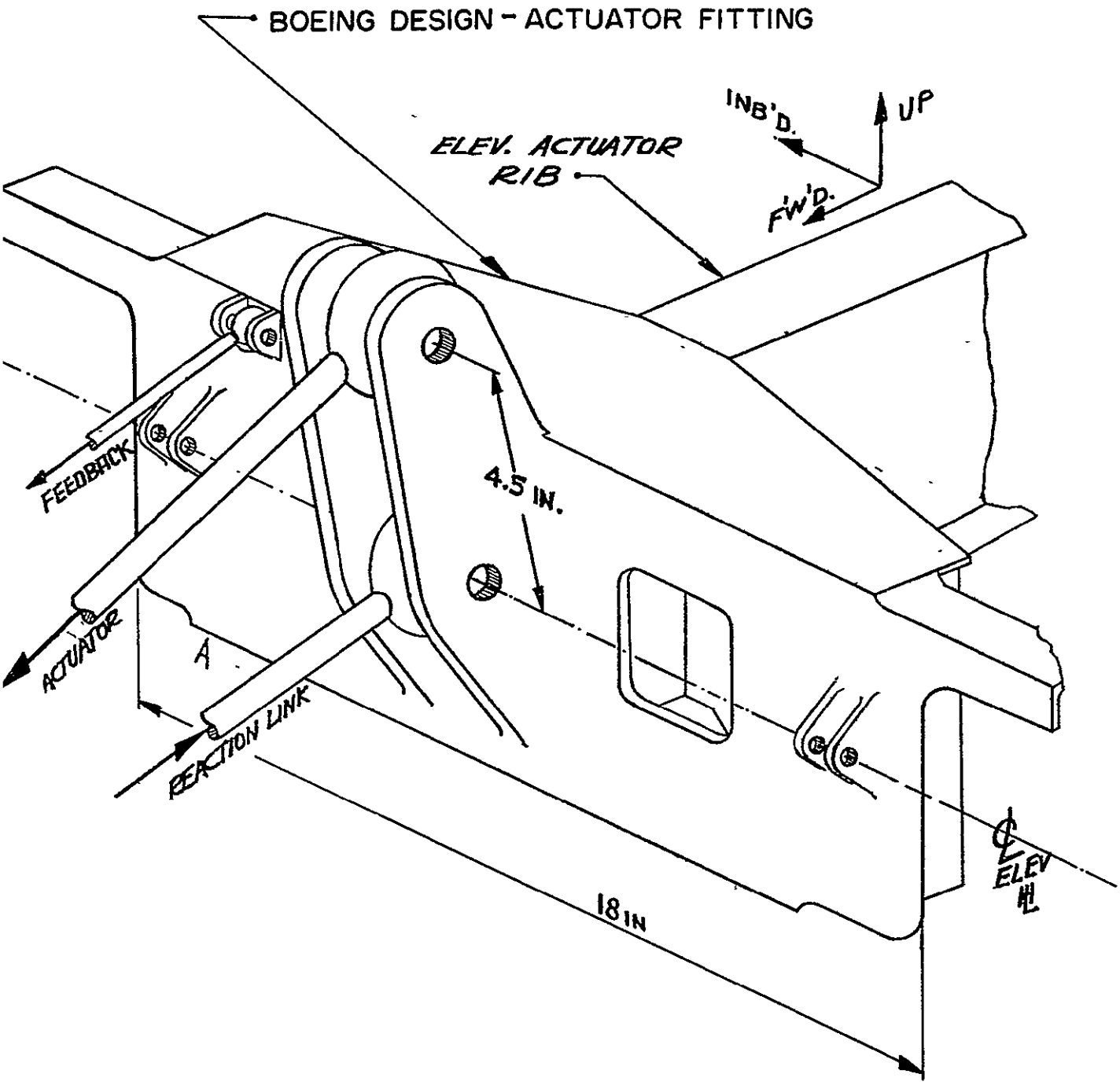
BOEING DESIGN - ACTUATOR FITTING
ELEV. ACTUATOR RIB
INB'D.
UP
FW'D.
FEEDBACK
ACTUATOR
REACTION LINK
4.5 IN.
A
18 IN
℄ ELEV HL

The shells were considered to be under uniform axial compression and composed of N orthotropic layers (Figure 6). Each layer was assumed to have the same thickness and an equal number of fibers in the $+\alpha_i$ and $-\alpha_i$ directions with respect to the longitudinal axis of the cylinder. The directions of the fibers in all the layers were sought which would give the highest buckling stress. A mathematical optimization technique (Powell's method) was applied to this problem.* The numerical calculations were made for a boron/epoxy composite.

Calculations were made for three-, four- and six-layered shells. The numerical results for 6-layered shells are shown in Table I. All of these cases are for a 6-layered circular cylindrical shell; the differences from case to case are due only to the starting configuration of ply angles. This table shows that better lamination angles than the starting values can be obtained by utilizing the optimization technique. Simple conclusions about the best lamination angles, however, cannot yet be drawn from the present results.

---

* A note related to this work has been accepted for publication in the Journal of Applied Mathematics.

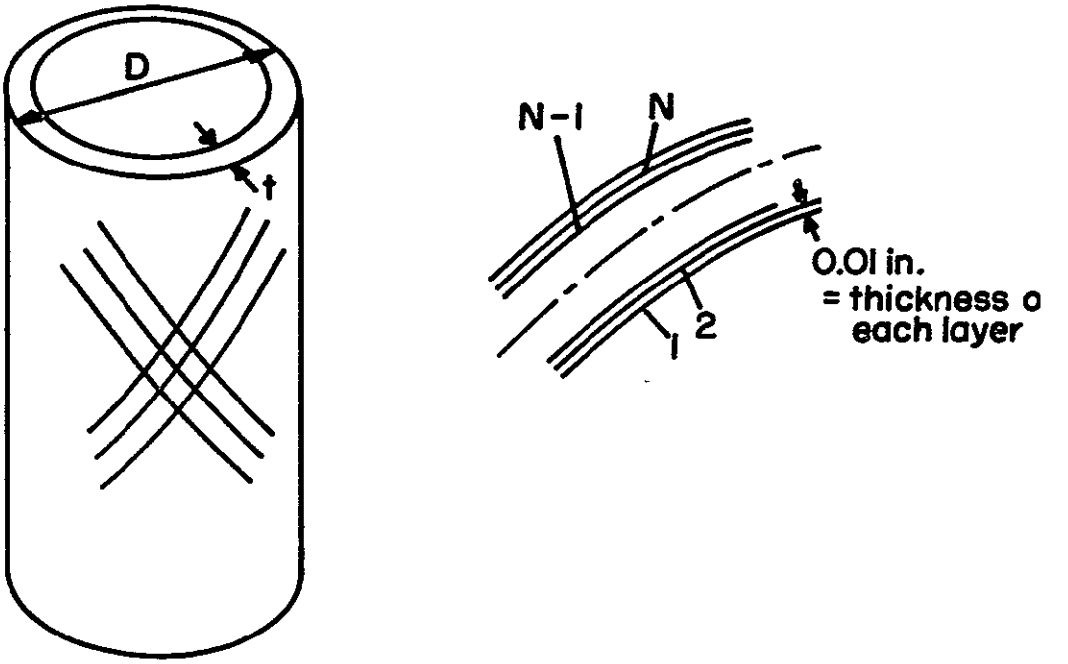

LAMINATED CYLINDRICAL SHELLS
Fig. 6

TABLE I - OPTIMUM FIBER DIRECTIONS FOR 6-LAYERED CYLINDRICAL SHELLS

Case		Fiber Directions (in degree) α_1	α_2	α_3	α_4	α_5	α_6	Reduced Critical Stress $\frac{\sqrt{3}}{2}\frac{D}{t^2}$Ncr (psi)
1	S	0.0	0.0	0.0	0.0	0.0	0.0	4.5785×10^6
	F	37.7	0.0	0.0	-34.8	35.2	43.2	1.0097×10^7
2	S	30.0	30.0	30.0	30.0	30.0	30.0	7.0029×10^6
	F	34.9	-0.0	-0.0	29.1	30.1	49.8	1.0131×10^7
3	S	45.0	45.0	45.0	45.0	45.0	45.0	5.9259×10^6
	F	45.0	45.0	45.0	45.0	45.0	45.0	5.9259×10^6
4	S	45.0	45.0	0.0	0.0	45.0	45.0	7.7602×10^6
	F	25.5	67.6	5.7	23.4	56.9	46.1	1.2278×10^7
5	S	0.0	0.0	45.0	45.0	0.0	0.0	7.5373×10^6
	F	37.0	8.1	86.9	-17.6	19.1	70.9	1.2150×10^7
6	S	90.0	90.0	90.0	90.0	90.0	90.0	4.5785×10^6
	F	136.3	90.5	90.4	187.6	106.8	215.5	1.2002×10^7
7	S	90.0	0.0	90.0	0.0	90.0	0.0	5.7750×10^6
	F	124.4	13.0	73.7	-1.7	90.6	30.0	1.2371×10^7
8	S	90.0	90.0	90.0	0.0	0.0	0.0	4.3848×10^6
	F	142.5	90.0	104.9	-5.2	57.4	45.2	1.2277×10^7
9	S	0.0	0.0	0.0	90.0	90.0	90.0	4.3848×10^6
	F	47.9	-3.1	-7.7	90.4	16.4	130.5	1.2057×10^7
10	S	10.0	20.0	30.0	40.0	50.0	60.0	7.4350×10^6
	F	24.3	-6.9	17.6	-0.6	0.5	72.1	1.0486×10^7

S: starting values

F: final optimum values

D: diameter of shell

t: thickness of shell

PART II

CAPGLIDE (Composite Aircraft Program Glider)

CAPGLIDE (Composite Aircraft Program Glider)

(E. J. Brunelle, R. J. Diefendorf,
H. J. Hagerup, G. Helwig and N. J. Hoff)

CAPGLIDE is an undergraduate program to design, build and test advanced composite structures. Students will obtain direct "hands-on" experience in advanced composite structures which can serve as a springboard for the more sophisticated CAPCOMP projects. In dealing with the design of a complete vehicle, the effect of any given change on other aspects must be dealt with. In this way the project also requires students majoring in aeronautical, mechanical and materials engineering to interact in much the same way as they do in industry.

An ultra-light sailplane was selected as the first demonstration project because a full scale flight vehicle would maximize student interest and would be of relative simplicity and low cost to build. A conventional layout monoplane with three axis control resulted in the following estimated performance:

1) Stall speed, 15 knots,
2) Best glide ratio, 17
3) Minimum sink rate, 2.0 feet per second.

While the glide ratio of the ultra-light sailplane is similar to that of post World War II utility gliders, the more important sink rate is in the range of standard class sailplanes.

The ultra-light sailplane project has moved into the detail design and fabrication phase. Student activity during the present contract period focused on detail design and analysis of the first version of the aircraft. Faculty and research staff supervised these efforts and, when student involvement decreased during the summer recess, also addressed the problem of modifying the original design to meet specifications. Such modification became necessary as early design estimates were replaced by more accurate predictions, achieved in part by the student design teams and in part through the addition to the project staff of fabrication specialists. The progress of the individual working teams is summarized as follows.

1. Pilot Accommodations and Control Fixtures - 5 students

The final full-scale mockup of the prone-pilot version of the aircraft center section has been fabricated. The mockup is complete, with operating control fixtures and pilot harnessing in place. The fully equipped mockup is ready for use in static and dynamic simulation of launch and landing procedures, for testing the layout and accessibility of the control fixtures in all pilot attitudes and for assessing overall quality and comfort of pilot accommodations.

2. Aerodynamics, Stability and Control - 6 students

Final and fully documented reports have been prepared on the longitudinal static stability, the longitudinal dynamics and the lateral stability and control of the original design. In addition to these results, an important achievement of this team is the development of a level of design and analysis competency on the part of its members normally not reached by students in our academic program until the senior and graduate years; yet the team is comprised mainly of sophomore and junior engineering students. This transfer of knowledge was effected by taking into the original team a mixture of sophomores and graduate students and by having the team together address the major design tasks in the stability and control area. The reports issued on the original design during the present contract period provide sufficient detail to allow incoming junior students to develop quickly the knowledge requisite to conducting similar calculations on future designs.

Specific results obtained on the basis of estimated stability derivatives and mass distributions for the original design are as follows, all reported as maximum L/D cruise unless otherwise stated: phugoid mode oscillatory with period 21 sec. and time to damp to half-amplitude 5 sec.; short period mode non-oscillatory, time to damp to half-amplitude 0.2 sec. (These results are consistent with the

low wing-loading and a mass-distribution concentrated near the center of gravity.); spiral divergence mode time to double-amplitude approximately 4.6 sec. at maximum L/D cruise with the pilot prone, and 3.2 sec. at landing with C_L = 1.70 and the pilot upright. These divergence rates are well within the pilot's capability to recover.

3. Design Modification - Faculty and Staff

Improved numbers on the structural weights of the aircraft became available in May, and two problems associated with the original design became evident: (1) The empty weight might significantly exceed 100 lbs. because of the need for sheets of adhesive and special connections in order to fabricate the honeycomb-sandwich D-box wing spar, and (2) the sweep angle of the wing might have to be increased to more than 12° with resulting performance degradation in order to maintain the static stability margins because of a 50% increase in the projected weight-and-balance estimate. Consequently, while the student design teams completed their analysis of the initial version, the faculty and research staff involved with the project during the summer recess reexamined the design and modified it substantially. The original D-box wing structure, starting at the wing leading edge, which carried both principle bending and torsion loads was replaced by a box-spar at 40% chord carrying primarily bending only. This change, with its farther aft

carry-through structure, permits the pilot now to be placed reclining with his shoulders within the forward root section of the wing. The necessity for wing sweep to achieve acceptable static margin was thus eliminated. For ease of fabrication, the wing was further made essentially untapered, with a tip-taper to minimize tip losses. Furthermore, wing area was reduced almost 20% to keep the weight down (see Figures 7 and 8). An open, lightweight fuselage shell was added around the reclining pilot to restore the performance lost in some of these changes. Whereas the earlier design depended on wing D-spar structure ahead of the pilot for nose impact protection, the new design uses an extension of the tail booms for this purpose (Figure 9).

With these general arrangement features chosen, a Computer Aided Design program used in Germany by Professor Gunter Helwig was employed to find the best compromise structure and wing planform. The first of these programs optimizes wing planform so that performance is maximized. The results of this program are used in a second program which calculates all wing loads and then performs a stress analysis especially devised for composite structures. Two separate algorithms deal with optimization and making the design one which employs fully stressed skin. The results from this second analysis are the thicknesses of the composite components and the angle orientations of the various plies. The final step in the design process is choosing

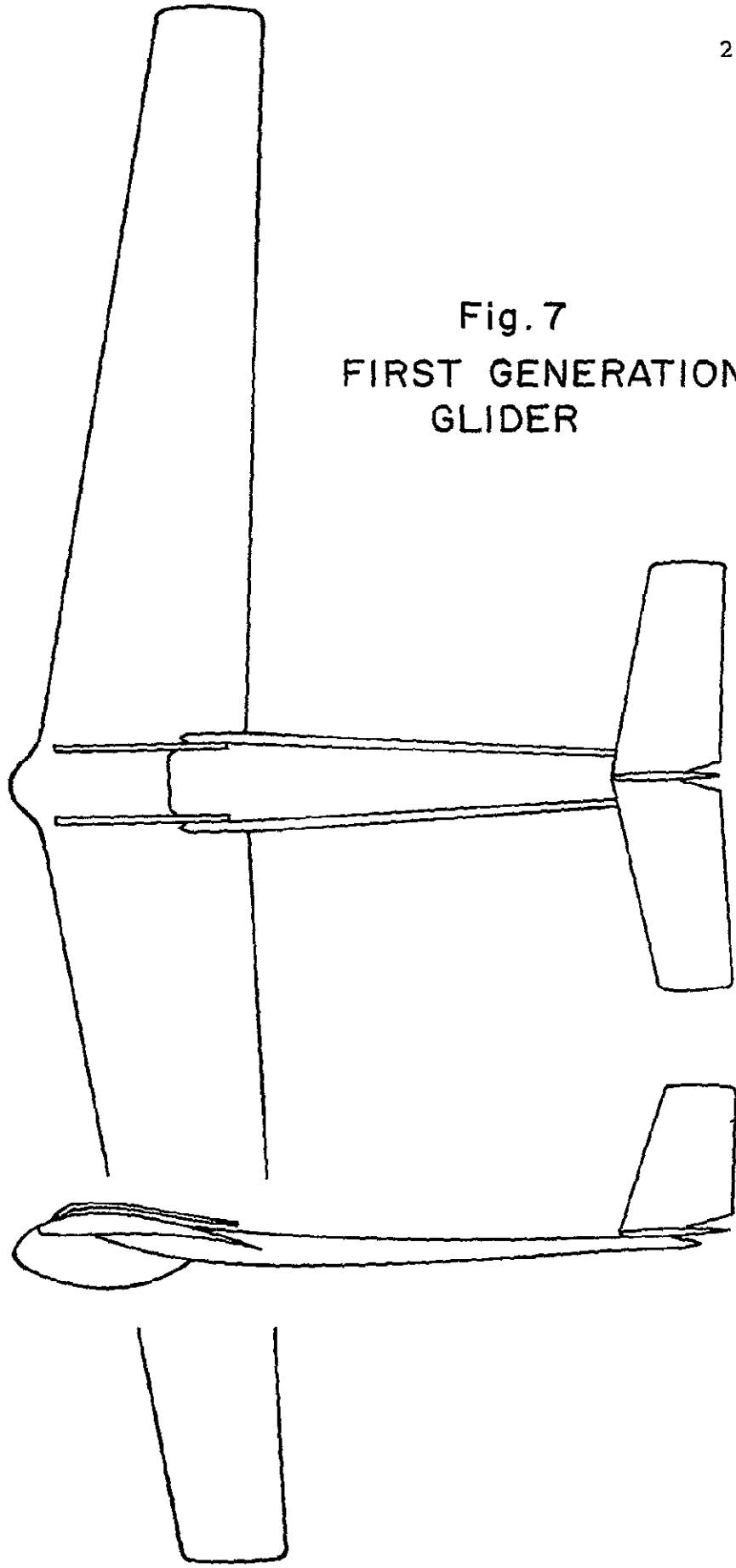

Fig. 7
FIRST GENERATION
GLIDER

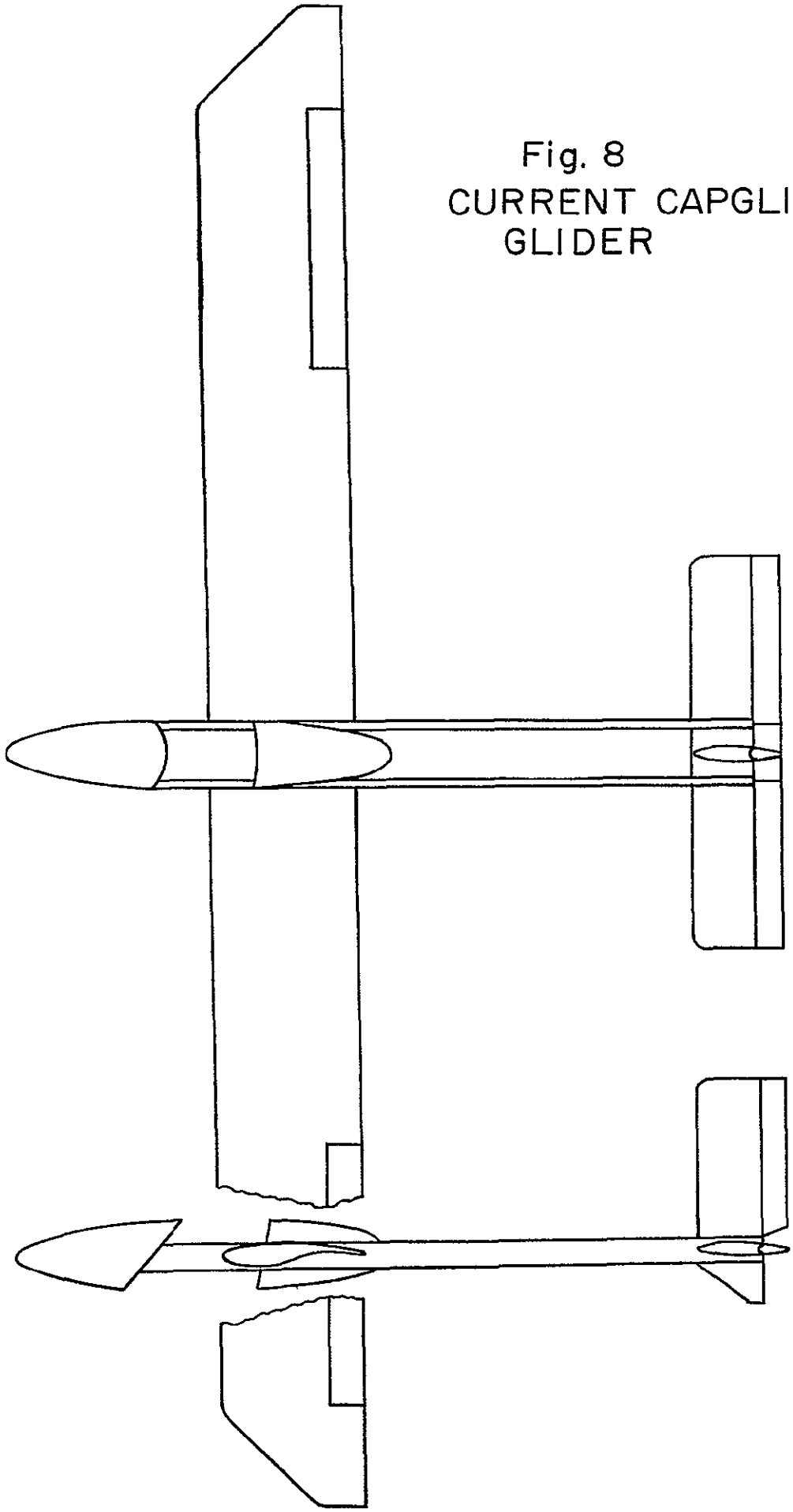

Fig. 8
CURRENT CAPGLIDE
GLIDER

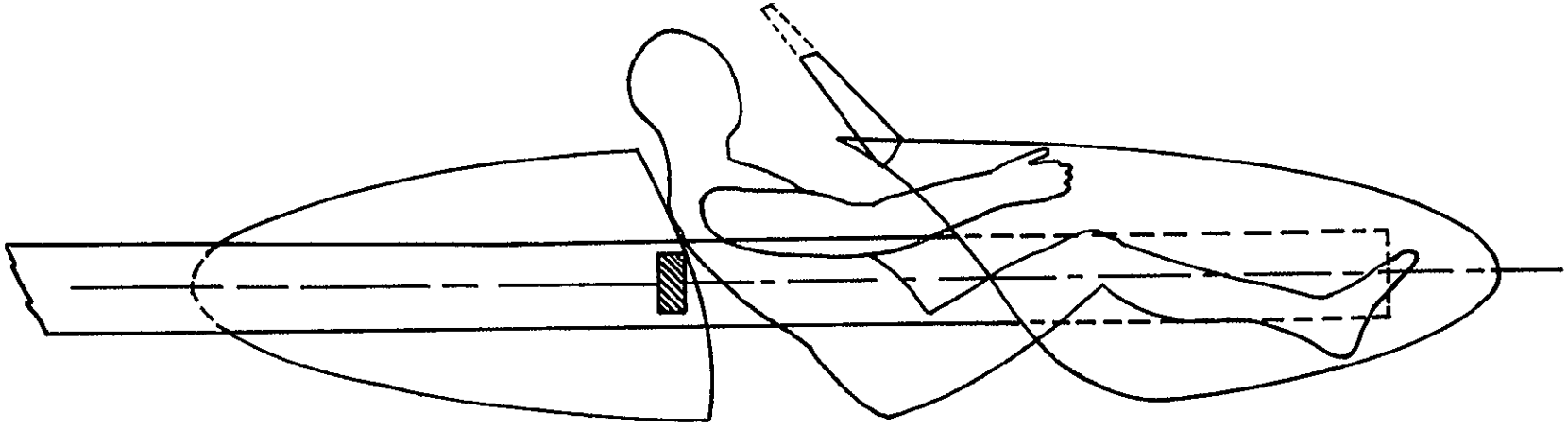

Fig. 9
PROPOSED FUSELAGE

fabrics from a catalogue to get the desired composite thicknesses. These three steps are shown schematically in Figure 10. The parameters possible for defining wing planform with this CAD program are shown in Figure 11. Although the untapered planform was desired, as mentioned earlier, for manufacturing reasons, a number of configurations were analyzed for comparative purposes, including the first generation CAPGLIDE wing, a completely untapered planform, the tip-tapered planform and another tapered arrangement. The basic wing structure is shown in cross-section in Figures 12 and 13 along with the various thicknesses possible for CAD analysis. Wing-fuselage connections and the associated means for load transfer are shown in Figure 14.

The results of the optimization study conducted using the CAD program are incorporated in the general design description shown in Figure 15.

The aircraft as modified in the new design remains a foot-launched ultra-light sailplane, with a cantilever stressed skin wing and a twin boom fuselage. The wing airfoil remains the Wortmann FX-136, and the performance characteristics will be similar to (and with respect to cross-country speed better than) those predicted for the original version, as shown in Table II using the definitions in Figure 16.

Fig 10

WING DESIGN WITH CAD

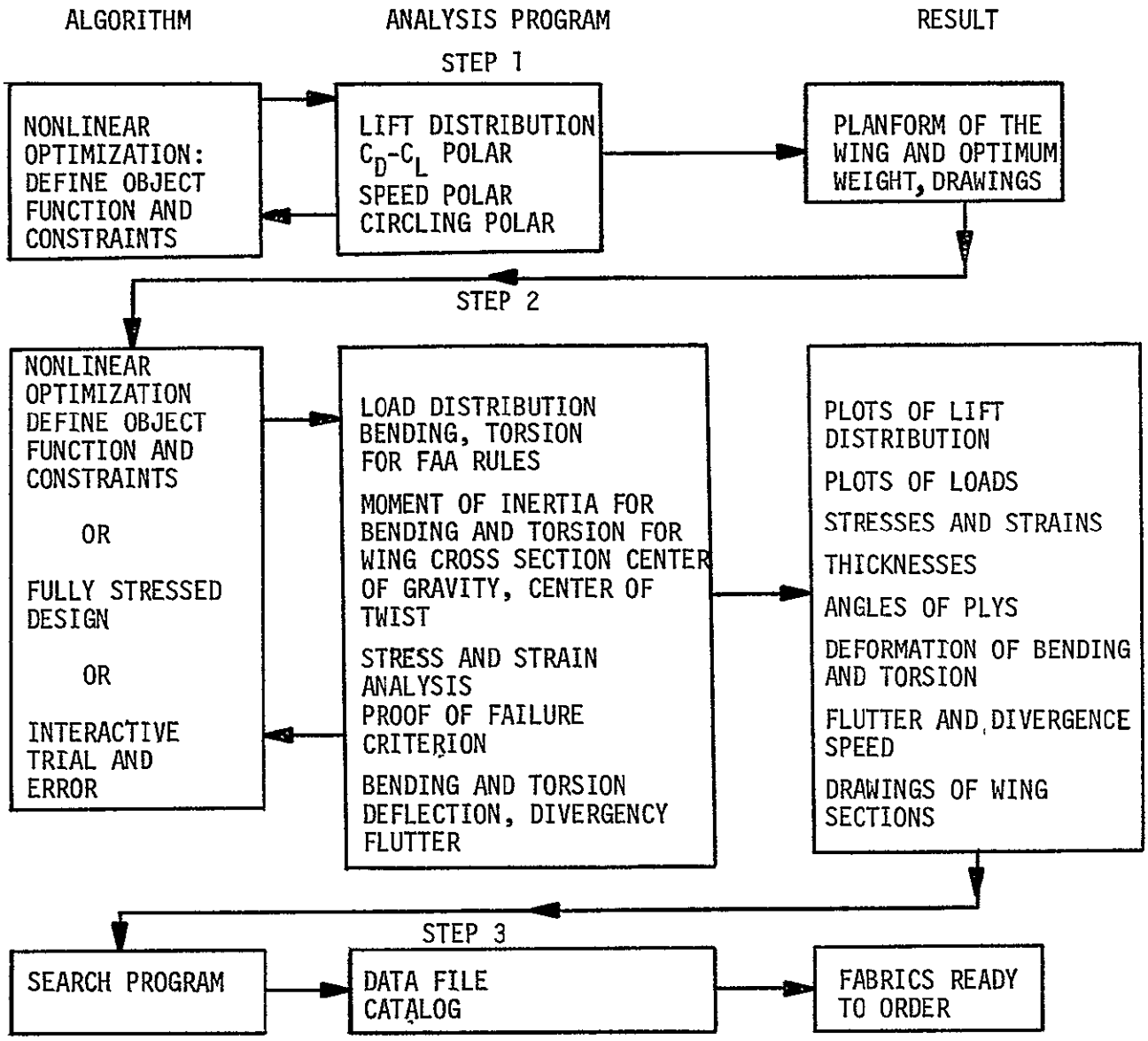

Fig. 11

PARAMETER FOR WING PLANFORM

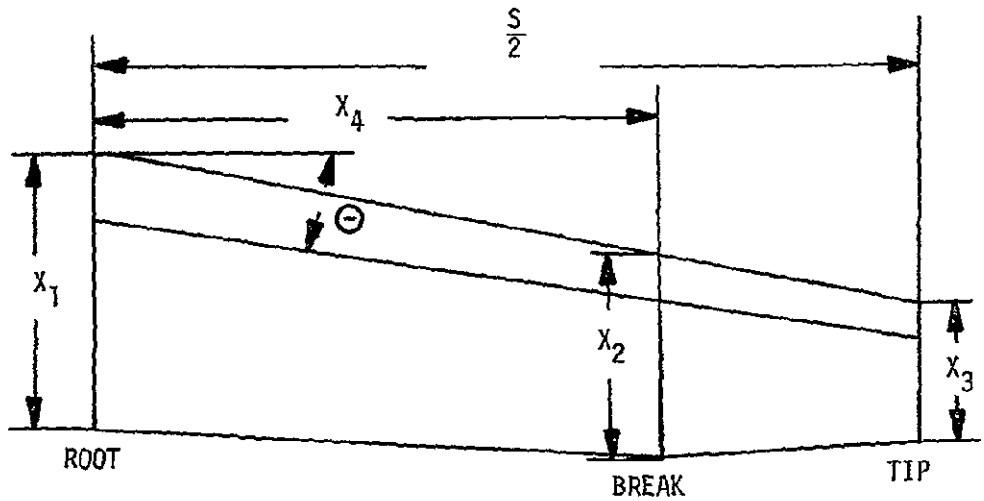

X_1 = CHORD AT THE ROOT

X_2 = CHORD AT THE BREAK

X_3 = CHORD AT THE TIP

X_4 = LENGTH TO THE BREAK

X_5 = INBUILT TWIST AT THE BREAK

X_6 = INBUILT TWIST AT THE TIP

X_7 = WEIGHT

S = SPAN (FIXED)

Θ = SWEEP ANGLE (FIXED)

Fig. 12 PARAMETERS OF THE WING SECTION

t_1 = THICKNESS OF UPPER SKIN

t_2 = " " " CORE

t_3 = " " LOWER SKIN

t_4 = " " " CORE

t_5 = " " WEB SKIN

t_6 = " " " CORE

t_7 = " " UPPER SPAR

t_8 = " " LOWER SPAR

t_9 = ANGLE OF UPPER SKIN LAYER

t_{10} = " " LOWER " "

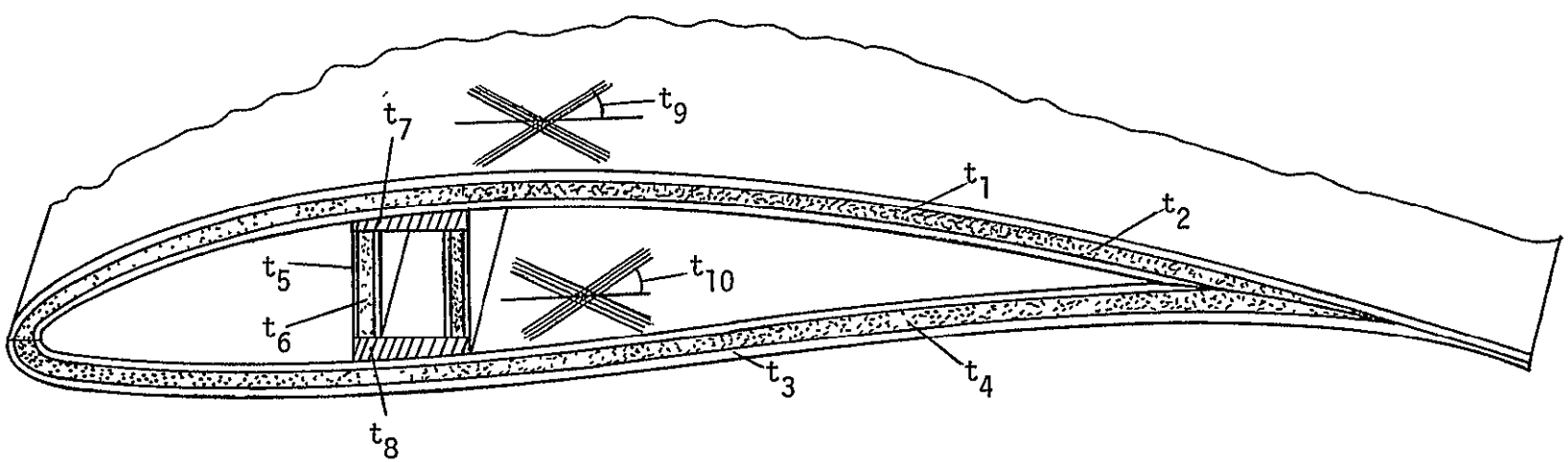

WING SECTION

Fig. 13

WING CONSTRUCTION

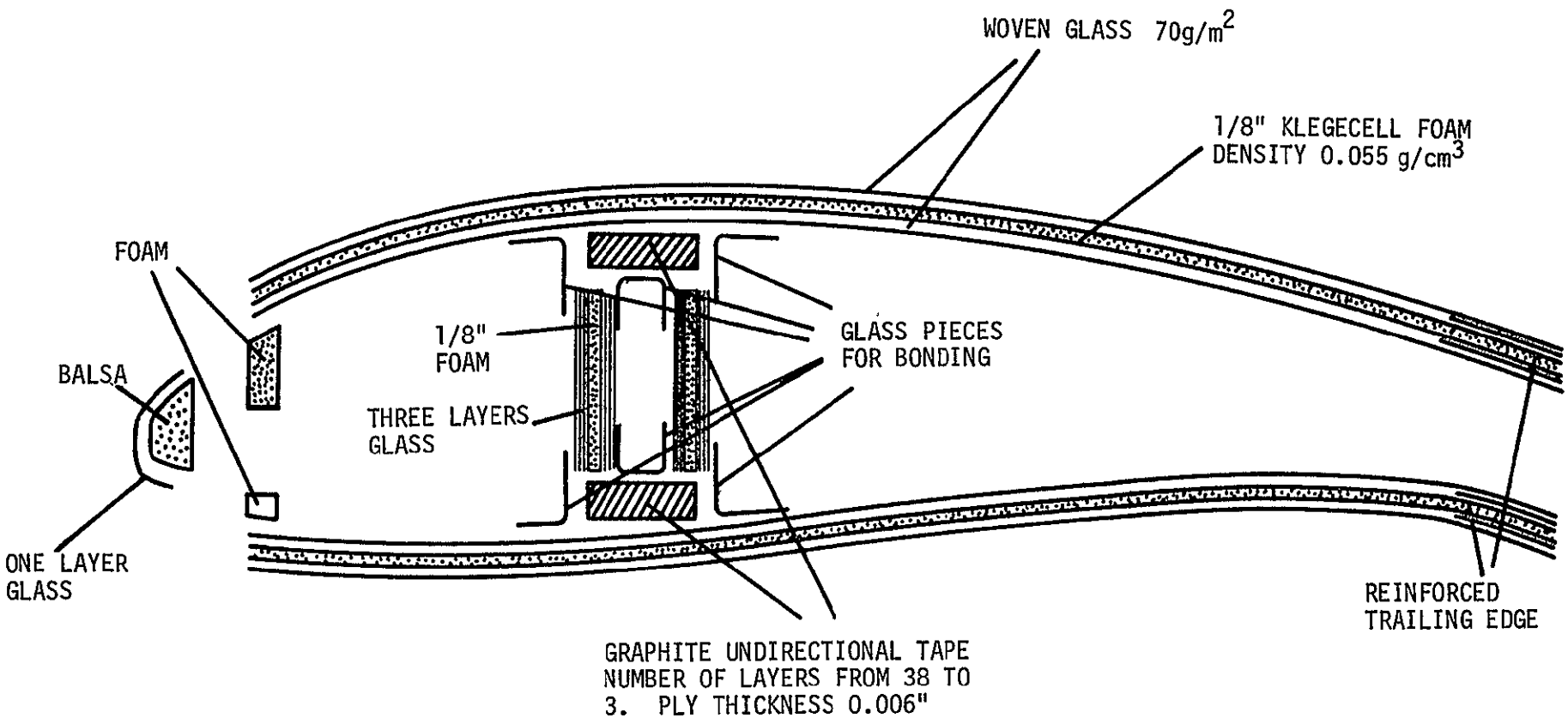

FOAM THICKNESS AND GLASS THICKNESS ARE CONSTANT.

REINFORCEMENTS AT THE ROOT, WING TIP, AND AILERON CONNECTIONS.

Fig. 14

WING CONNECTION

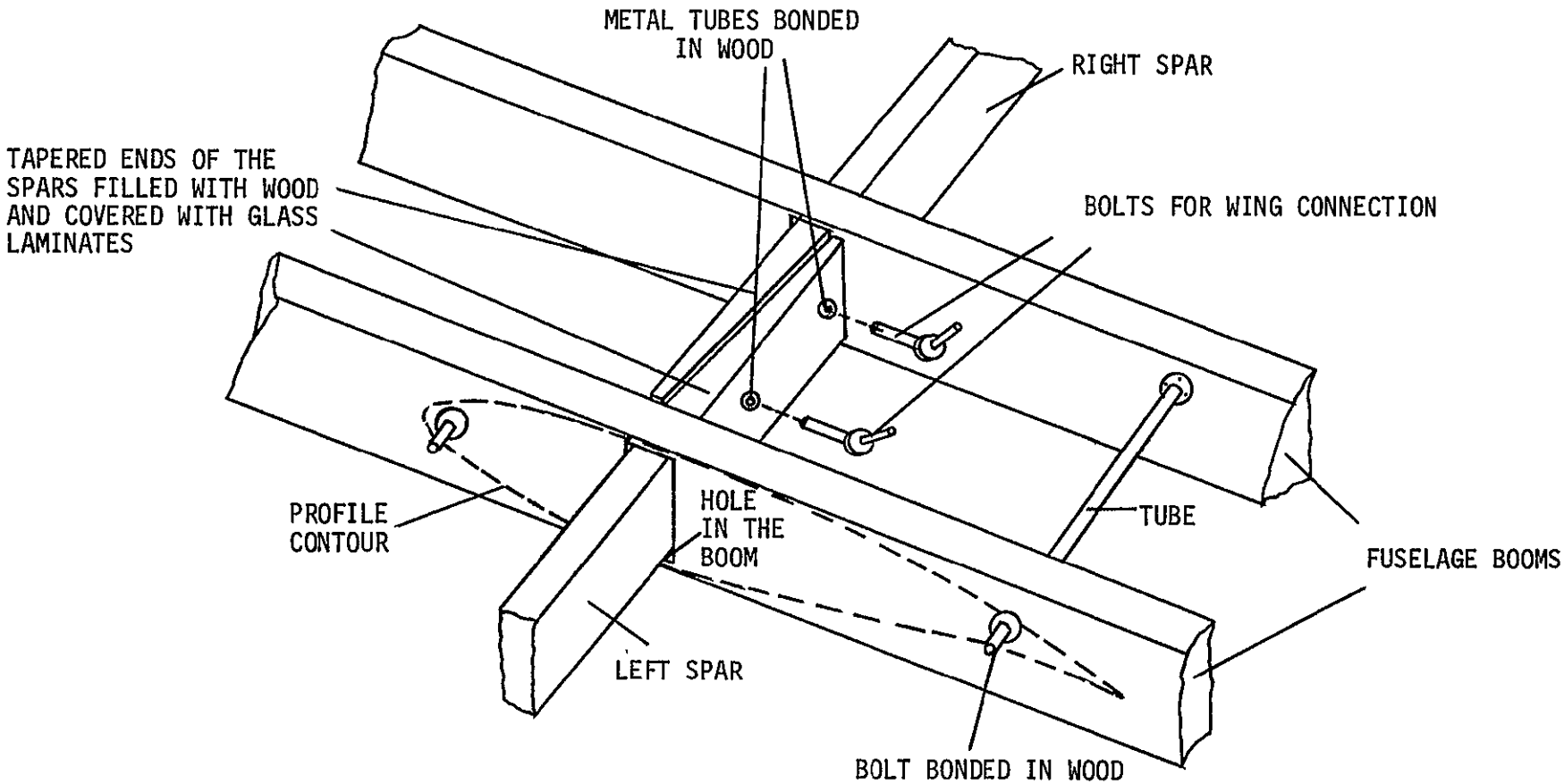

THE COMPOSITE COMPONENTS IN CAPGLIDE

Fig.15

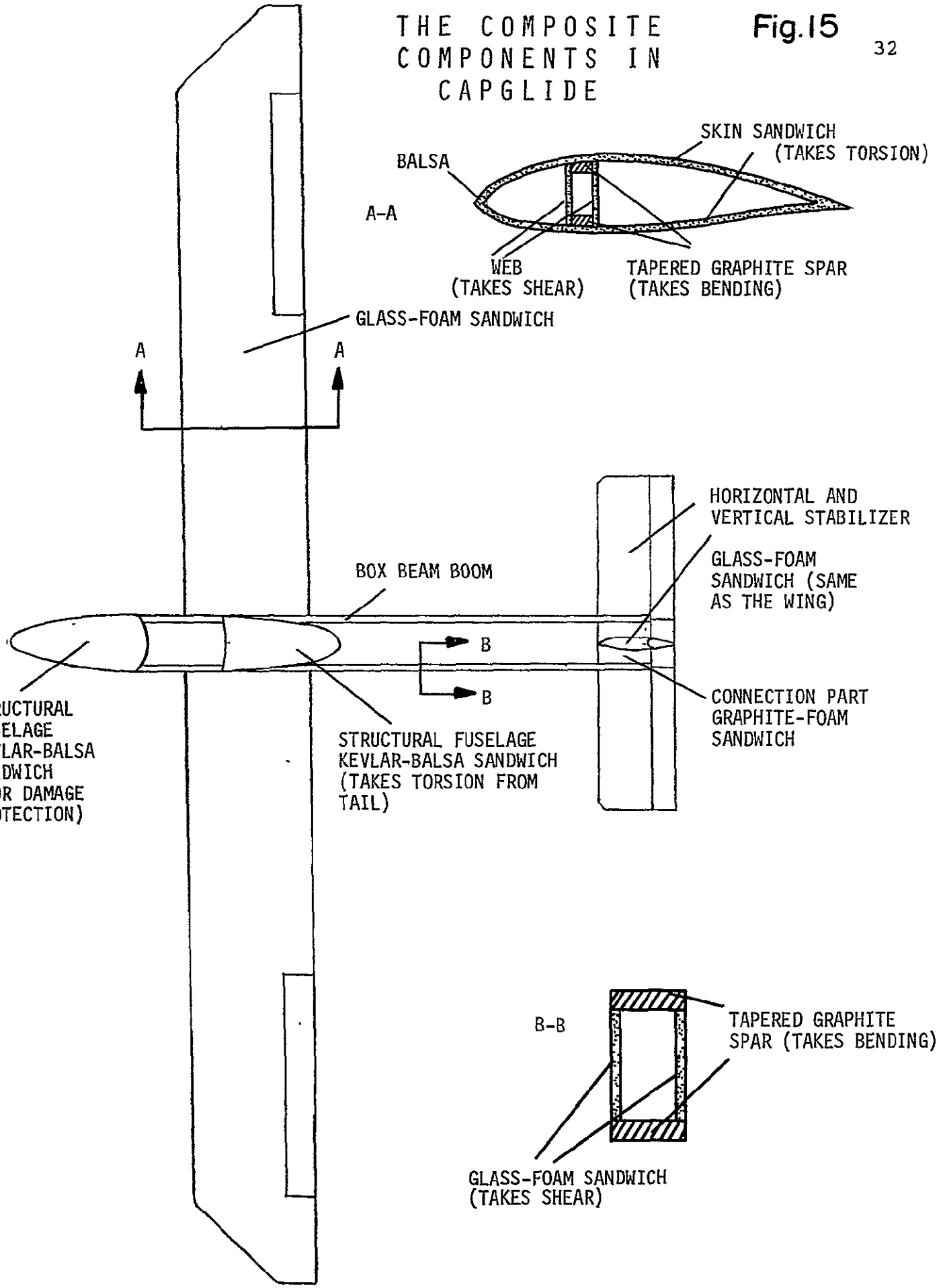

TABLE II
DESIGN ALTERNATIVES
PERFORMANCE COMPARISONS

Characteristic \ Planform*	1 Old	2 New	3 Other	4 Other	Dimension
Span	12.2	11.5	11.5	11.5	m
Area	14.8	12.0	12.0	12.0	m^2
Aspect Ratio	10.0	11.0	11.0	11.0	-
$(C_L/C_D)_{max}$	21.22	20.42	19.85	20.67	-
Minimum Sink	0.567	0.624	0.642	0.613	m/s
Cross Country Speed	52.55	53.74	53.00	53.96	Km/h
Stall Speed	33.0	36.0	36.0	36.0	Km/h

Change in Performance Between Cases	1-2	2-4	3-4	4-4
$(C_L/C_D)_{max}$	+3.92%	-1.21%	-3.97%	0.0%
Minimum Sink	-9.13%	+1.79%	-4.37%	0.0%
Cross Country Speed	-2.21%	-0.41%	-1.78%	0.0%
Stall Speed	-8.33%	0.0%	0.0%	0.0%

* Weight for all is 120 kg.

Fig. 16
PERFORMANCE CRITERIA

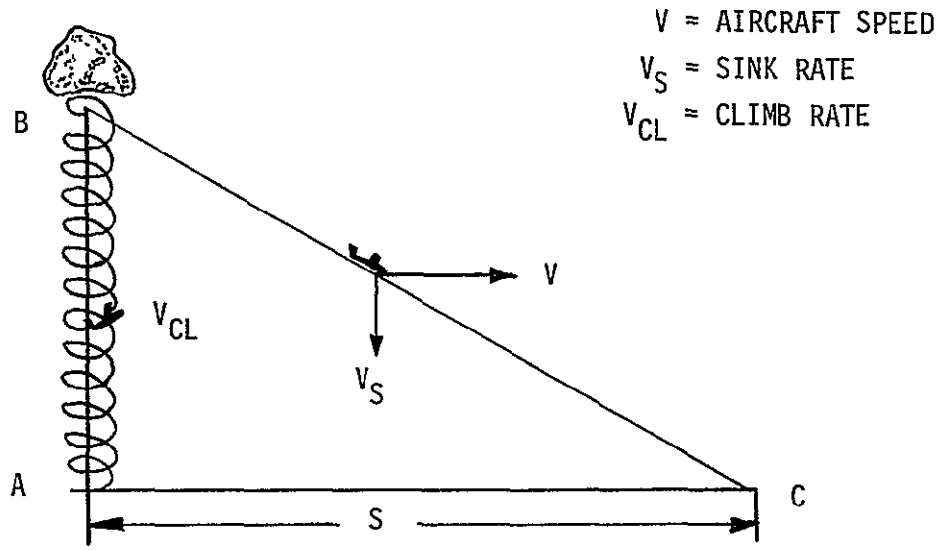

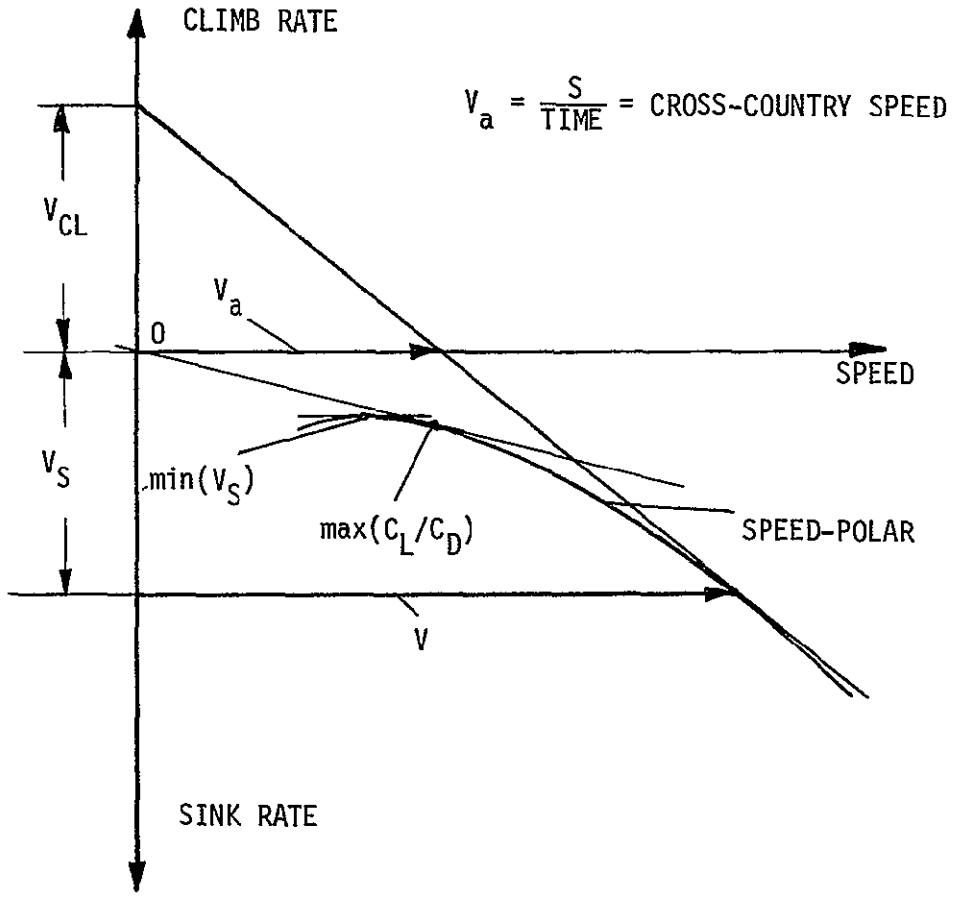

4. Aeroelastic Studies

A. Introduction and Overview

This reporting period began with the routine procedures necessary for the analysis of classical binary wing flutter, boom-tail flutter and control surface flutter being performed.

There has been continuing concern for the boom design problem, in general, and a growing doubt that any of the various classical analyses would be valid indicators of a flutter-free glider, since the large tail loads strongly hinted that the critical flutter speed would involve the complete aircraft motion including its rigid body motions in plunge, pitch and roll. This doubt was reinforced at the Eighth U. S. National Congress of Applied Mechanics Meeting held at UCLA in late June, 1978. The Aeroelasticity Session Chairman (Professor Peretz Friedmann of UCLA), during a visit with E. J. Brunelle*, related the following set of events:

> Several years ago the National Israeli Aircraft Establishment designed and fabricated a prototype twin-boom cargo aircraft. All the usual flutter calculations yielded satisfactory results, yet the prototype crashed, killing all crew members. A more careful flutter analysis that included the

---

* E. J. Brunelle presented a paper in Professor Friedmann's Session entitled "Some Aeroelastic Pathologies of an Ultralightweight Graphite/Epoxy Glider", (sponsored by the subject NASA Grant, No. NGL 33-018-003).

> effects of large concentrated torques introduced into the wings (via the booms due to the tail loads) revealed an unusually low flutter speed. Needless to say a major redesign was necessary.

While the above-mentioned cargo aircraft and our glider are largely dissimilar in geometry and extremely dissimilar in mass distribution and flight envelope characteristics, both aircraft have tail loads large with respect to their wing loads, which in turn impose large concentrated torques into their wing structure. This <u>is</u> a disturbing common feature and - along with the previously reported low values of $U_F/b\omega_\alpha$ and μ (the reduced flutter speed and the mass-density ratio) for the binary flutter models of our glider wing - should sound a strong cautionary note. Furthermore, this cautionary note should be heeded not only as regards flutter and dynamic response aspects of our glider, but also as regards its static stability and control, only limited aspects of which have been checked for aeroelastic effects. Previous calculations for $\partial C_m/\partial\alpha$ (both stick-fixed and stick-free) showed a 13 to 32 percent reduction* due to tail boom deflection alone at the 100 ft./sec. "penetration speed" condition, without load factor being included. One extreme

---

* The 13% figure assumed 8" constant diameter 6-ply construction, and the 32% figure assumed 5.5" constant diameter 6-ply construction (these booms were purposely oversized to demonstrate a persisting significant effect). A value of $E = 11 \times 10^6$ psi was used and the ply thickness was taken to be .005 inches.

right-hand portion of the V-N diagram has a load factor, N, equal to 8.0 (5.4 x safety factor of 1.5).

Accordingly, the following necessary priority areas have been formulated for investigation:

(i) A mathematical flutter model for the glider will be derived which includes all relevant body motions and describes the tail/tail-boom wing interaction process.

(ii) A solution technique will be devised that is both informative for students (i.e., a solution method that imparts some physical meaning of the flutter mechanism) and sufficiently accurate. The technique must not be expensive and time consuming.

(iii) The effects of aeroelastic deformation on all of the significant static stability and control problems will be carefully explored to dispel or draw attention to some current doubts.

(iv) If warranted, after the results of Section (iii) are known, the effects of aeroelastic deformation will be included in the performance equations to yield revised estimates of range and rate of sink (particularly) at the "penetration glide" condition.

B. Static Stability and Control Problems; Rate of Sink and Range Problems

During the last period expressions given in texts dealing with the static longitudinal stability and control of rigid aircraft [such as Perkings and Hage (1949), Etkin (1959) and (1972), etc.] were rewritten in a form which

would allow study of aeroelastic effects on stability control. These results, when combined with the elastic degree of freedom equations, provided the expressions needed to calculate the desired effects.

In brief, the equations

$$L_{WING/BODY} + L_{TAIL} = NW$$

$$M_{C.G.} = 0$$

provide constraint equations* that enable the elastic variables to assume specific values. The elevator hinge moment equation (with its added aeroelastic terms) provides an auxiliary equation to calculate trim tab angles, elevator floating angles, etc., but most importantly to calculate stick forces and stick force gradients. With much more labor than is characteristic of rigid aircraft analysis, it is then possible to calculate the following quantities for elastic aircraft:

(i) $\partial C_m/\partial\alpha$; stick-fixed and stick-free.
(ii) The stick-fixed and stick-free neutral points.
(iii) Coupled values of wing reference angle and elevator angle to "trim" for a given speed and load factor N.

---

* In rigid aircraft analysis these equations immediately yield the "trim values" for the wing angle of attack and the elevator angle. Aeroelastic effects are a complicating factor.

(iv) Stick forces to "trim"; trim tab angles to eliminate stick forces at given flight speeds.

(v) Stick force gradients.

(vi) Stick force per g.

(vii) Elevator angle per g.

With some more labor it is then possible to calculate the aeroelastically modified rate of sink and range values for any desired speed and to calculate the minimum sink rate, the maximum range (and their respective speeds)*.

Much of the theoretical work has been completed; it must now be checked for errors. Some calculations are proceeding with updated values of parameters furnished by the aerodynamics group.

Late in the reporting period, general comparisons of old and new design aeroelastic characteristics were made. Some of the results are shown in Figures 17 through 25.

C. Flutter Involving Complete Aircraft Motion

The last two working weeks of the summer and the beginning of the fall term were spent formulating a flutter model. The current avenue of exploration utilizes quasi-steady (or quasi-unsteady) aerodynamics and assemblages of one-dimensional influence functions (to approximate the influence function for the "plate-like aircraft" used by

---

* The performance equations uncouple from the static stability and control equations only if the glide angle β is shallow enough that $\beta \cong \beta$ and $\cos \beta \cong 1$.

Fig. 17

COMPARISON OF OLD AND NEW

TYPICAL SECTION WING ANALYSIS

$$\frac{\partial C_L/\partial\alpha}{(\partial C_L/\partial\alpha)_{R.W.*}} = \frac{1}{1 \mp Q}$$

Where: $-$ corresponds to $e > o$

$+$ corresponds to $e < o$

$$\text{AILERON EFF.} \equiv \frac{\partial C_L/\partial\beta}{(\partial C_L/\partial\beta)_{R.W.}} = \frac{1 - Q/Q_R}{1 \mp Q}$$

Where: $Q = q/q_1$

q = Dynamic Pressure

$$q_1 = \frac{k}{S\,|e|\left(\frac{\partial C_L}{\partial\alpha}\right)_{R.W.}}$$ for either sign of e

$\equiv q_D$ (Divergence Dynamic Pressure) for $e > o$

S = Wing Area

$Q_R = q_R/q_1$

q_R = Aileron Reversal Dynamic Pressure $= \dfrac{-(\partial C_L/\partial\beta)_{R.W.}}{(\partial C_{m_{a.c.}}/\partial\beta)_{R.W.}} \dfrac{|e|}{c'} q_1$

$$\frac{(A.E.)_{e<o}}{(A.E.)_{e>o}} = \frac{1 - Q}{1 + Q}$$

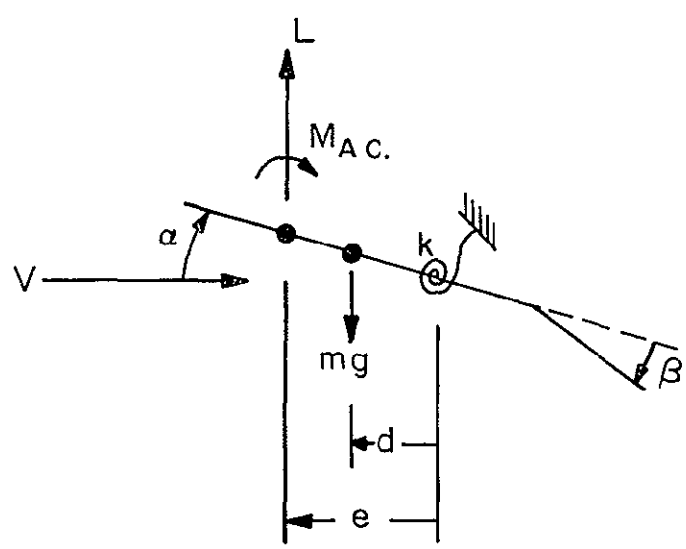

* Rigid Wing

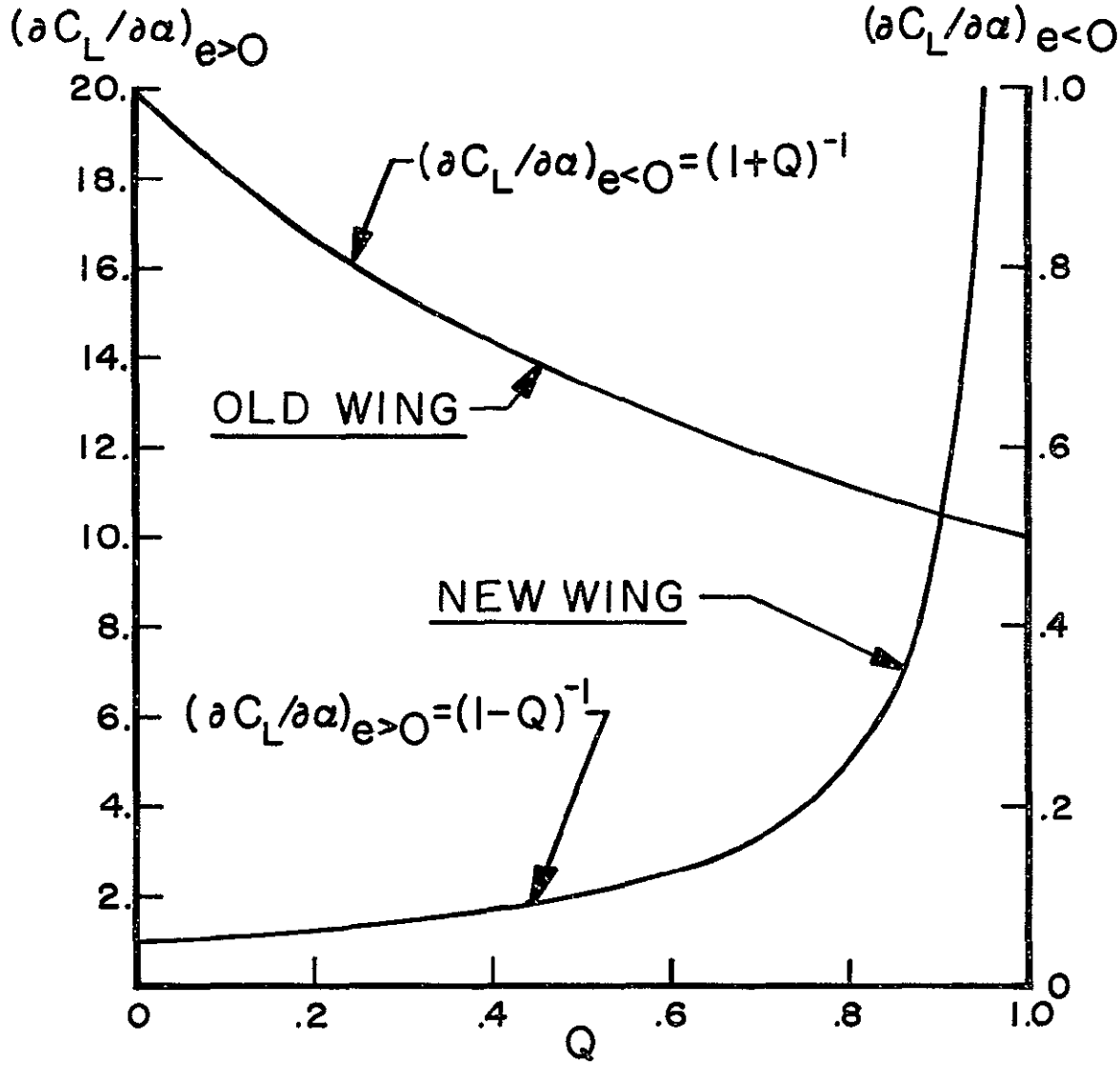

$\partial C_L/\partial\alpha$ VS. Q FOR e>0 AND e<0

FIG. 18

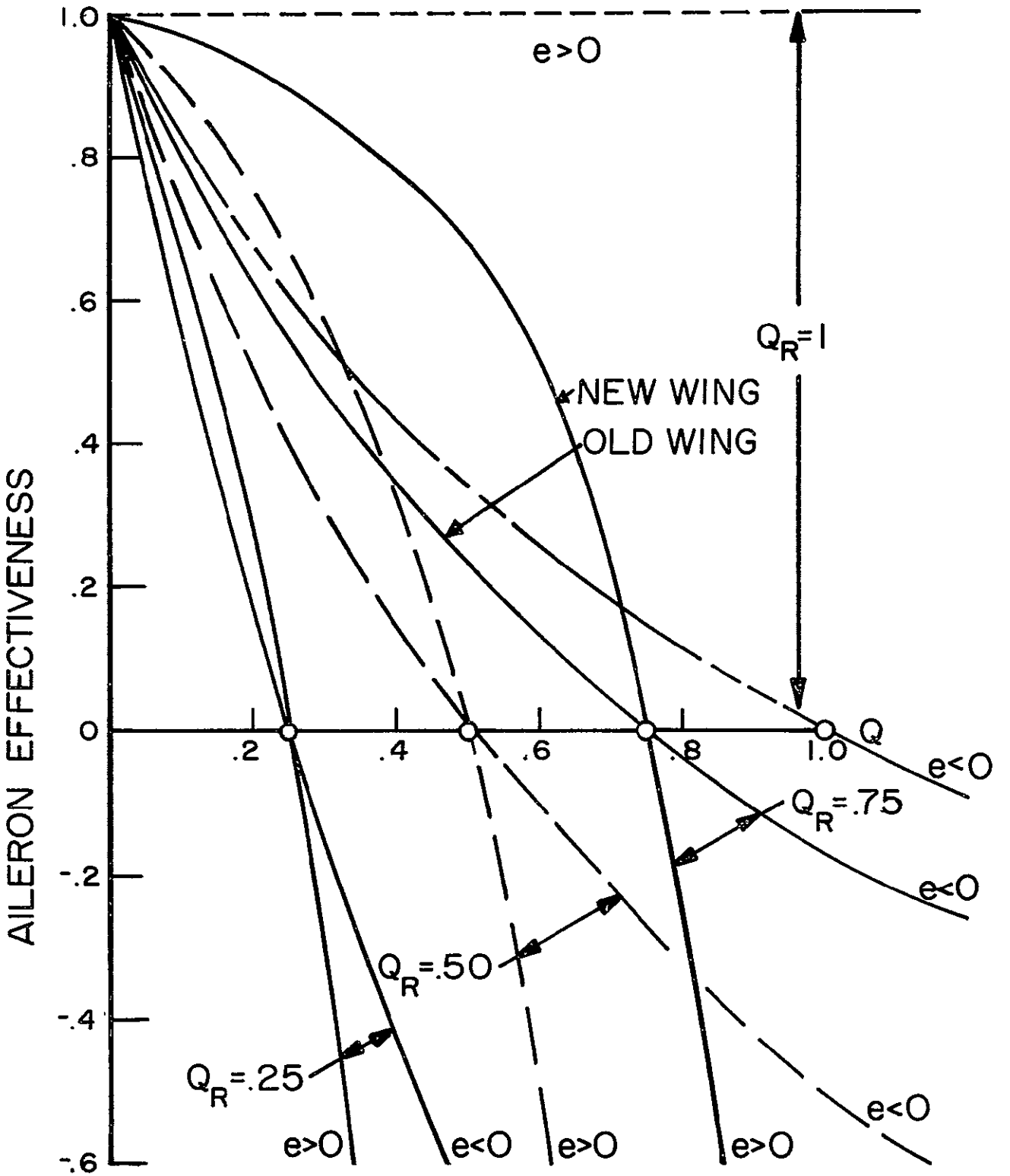

AILERON EFFECTIVENESS VS. Q WITH Q_R AS A PARAMETER (FOR BOTH e>0 & e<0)

Fig. 19

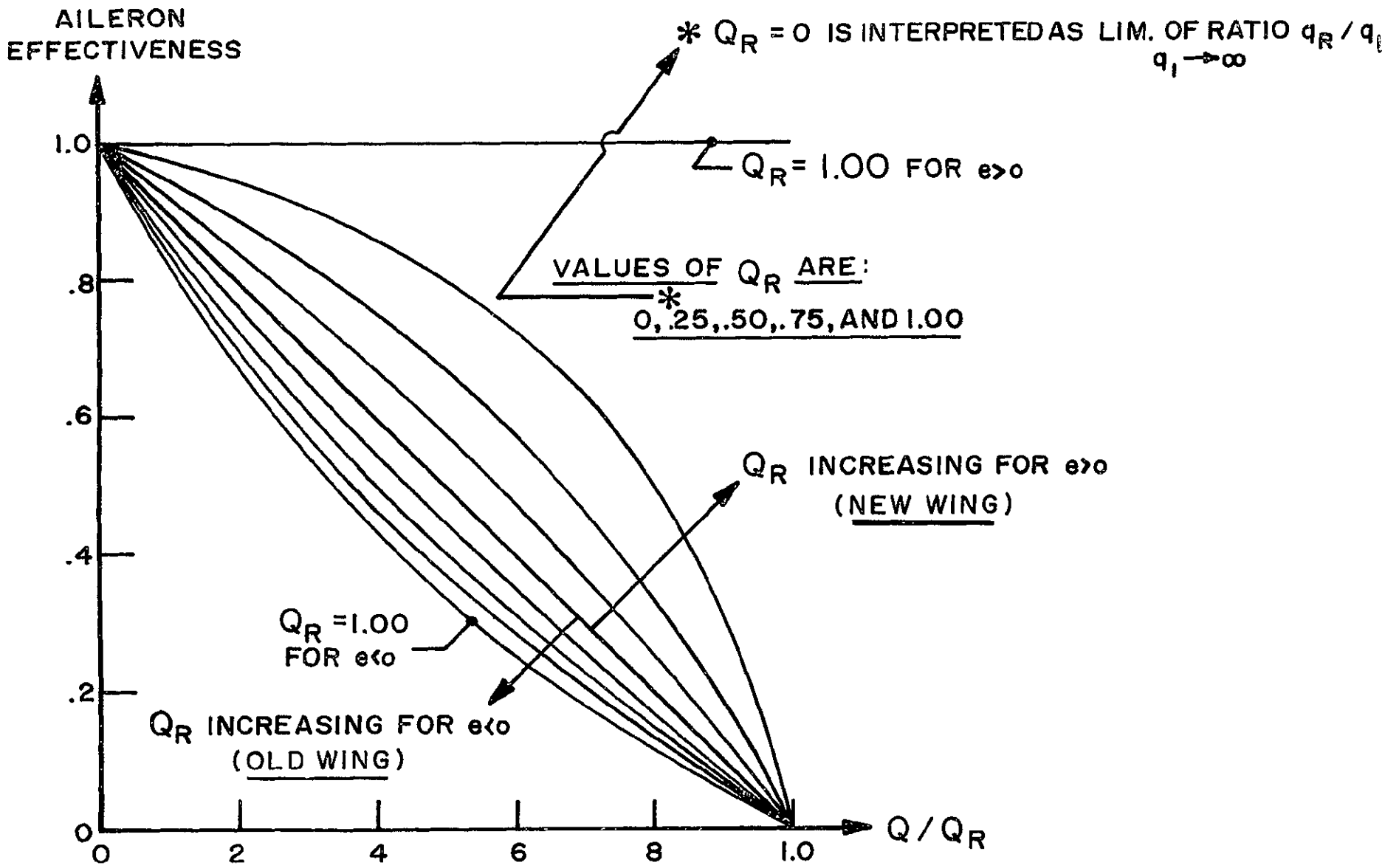

AILERON EFFECTIVENESS VS. Q/Q_R WITH Q_R AS A PARAMETER

Fig. 20

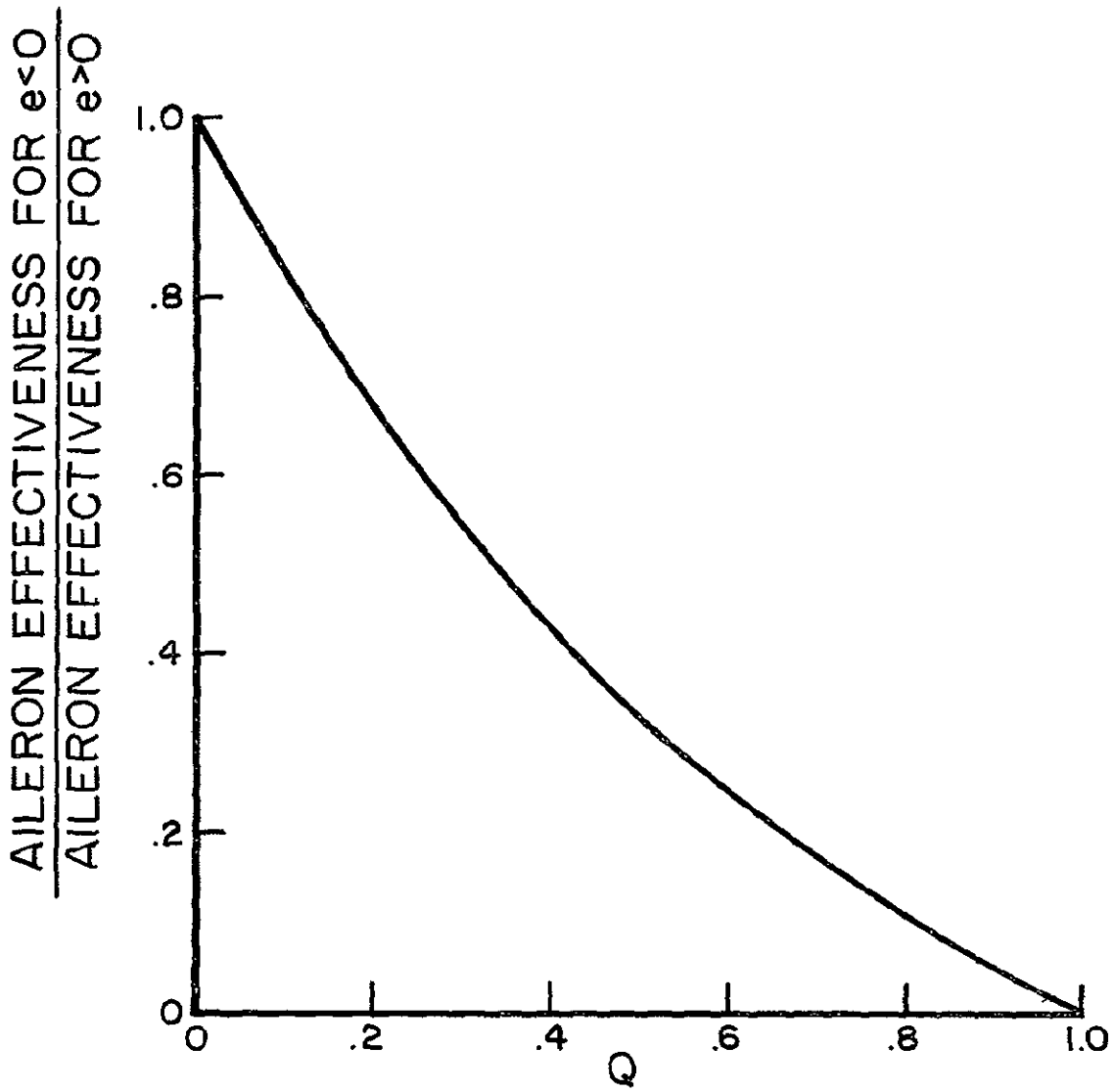

$\left[\frac{\text{OLD WING A.E.}}{\text{NEW WING A.E.}} \text{ VERSES Q}\right]$

Fig. 21

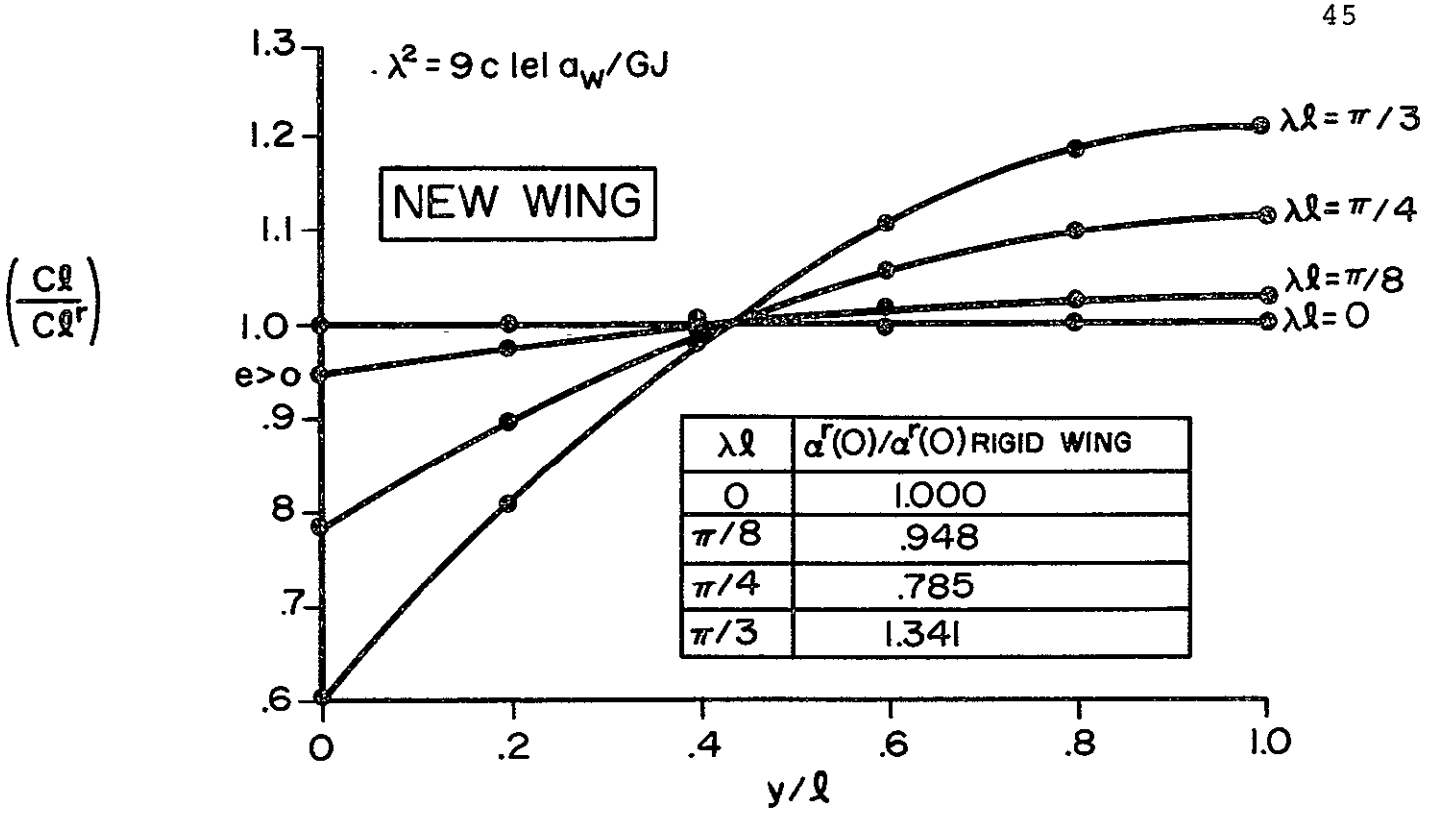

$\lambda\ell$	$\alpha^r(0)/\alpha^r(0)$ RIGID WING
0	1.000
$\pi/8$	.948
$\pi/4$	.785
$\pi/3$	1.341

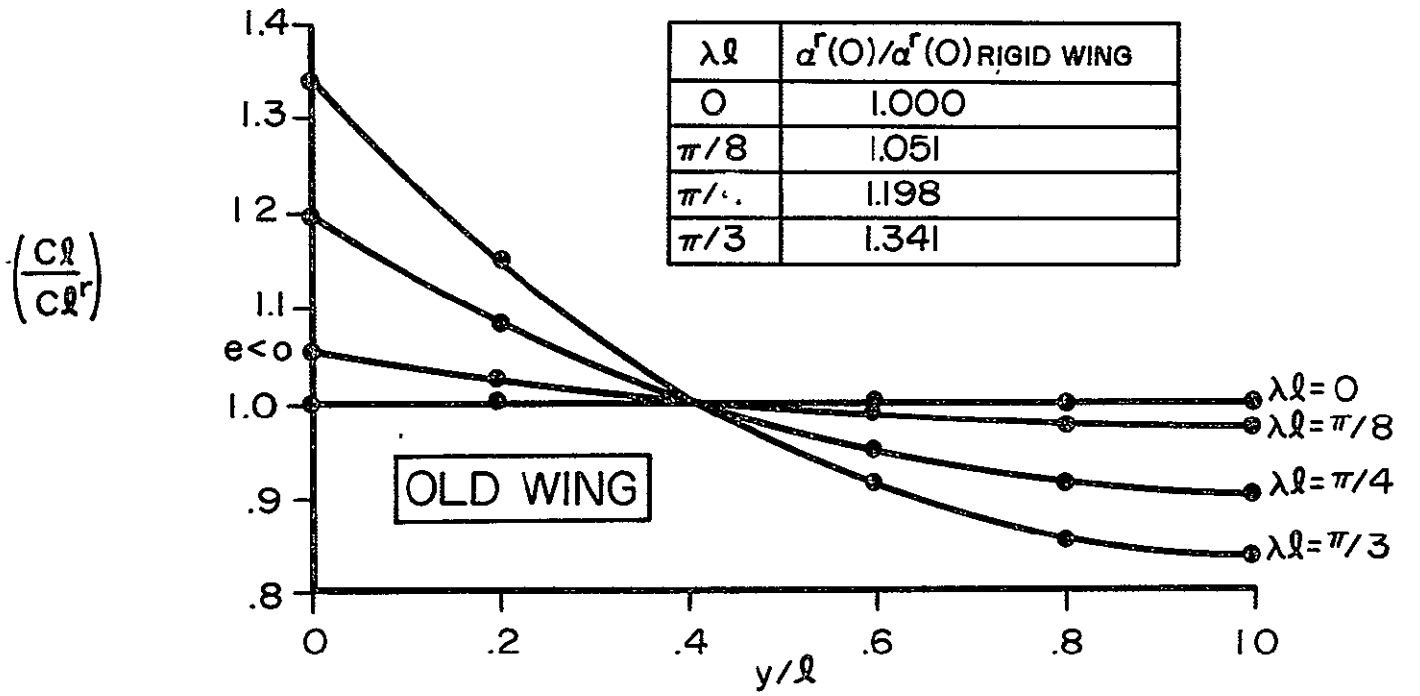

$\lambda\ell$	$\alpha^r(0)/\alpha^r(0)$ RIGID WING
0	1.000
$\pi/8$	1.051
$\pi/4$	1.198
$\pi/3$	1.341

LIFT REDISTRIBUTION ON UNIFORM WING (Cmac = d = o) WITH LOAD FACTOR N SPECIFIED FOR e>o AND e<o

Fig 22

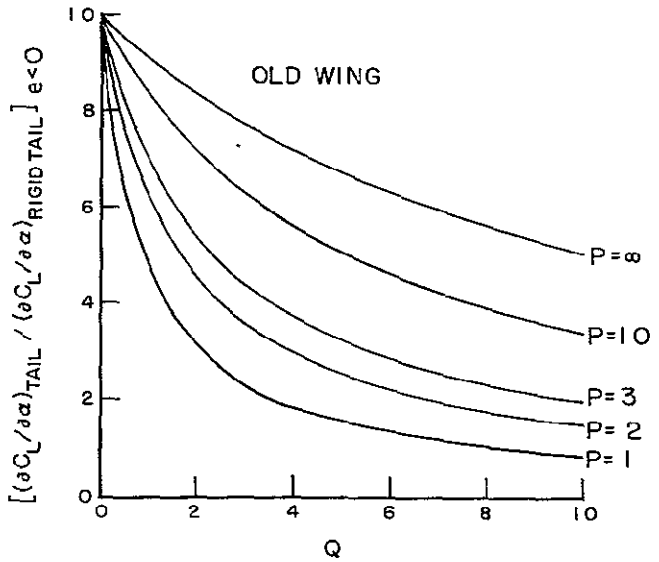

C_T^* FOR D-BOX TAIL VS Q

Fig 23(a)

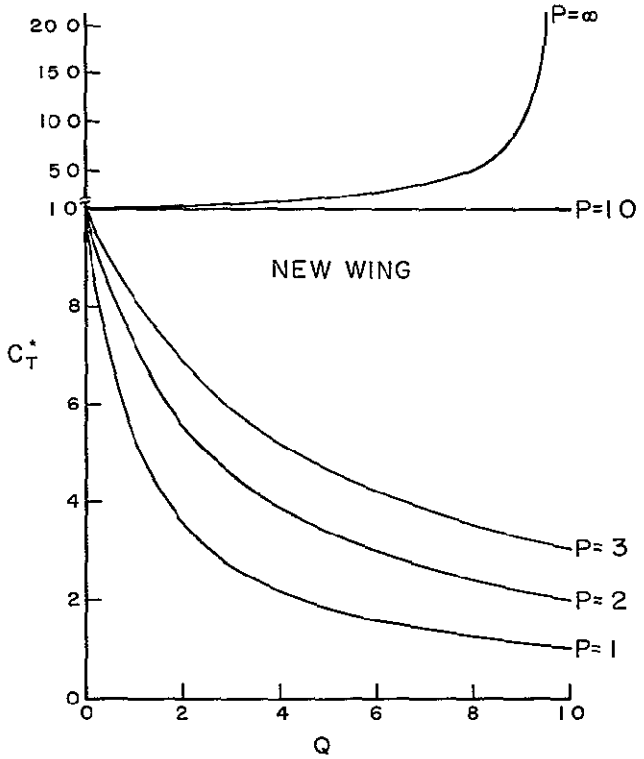

C_T^* FOR USUAL TAIL CONSTRUCTION VS Q

Fig 23(b)

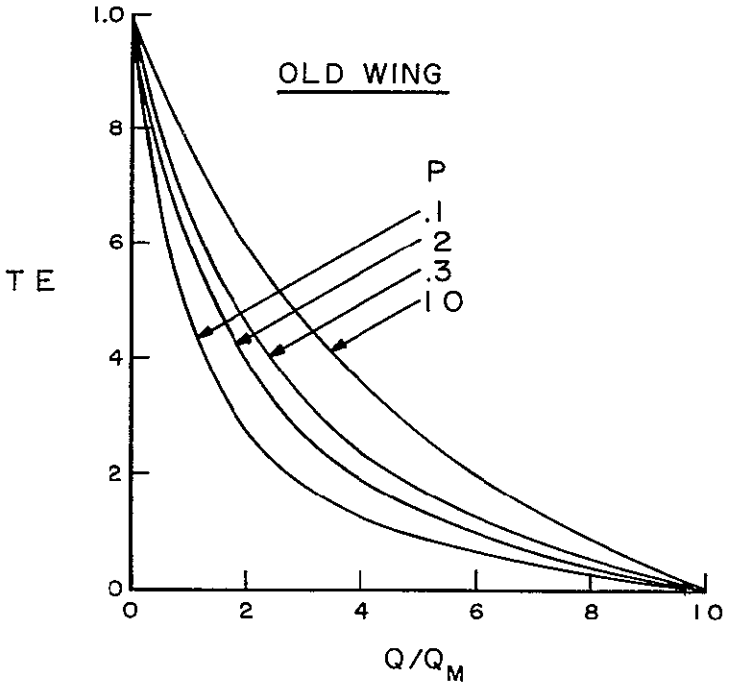

TAIL EFFECTIVENESS VS Q/Q_M
($e_t < 0$)
Fig 24 (a)

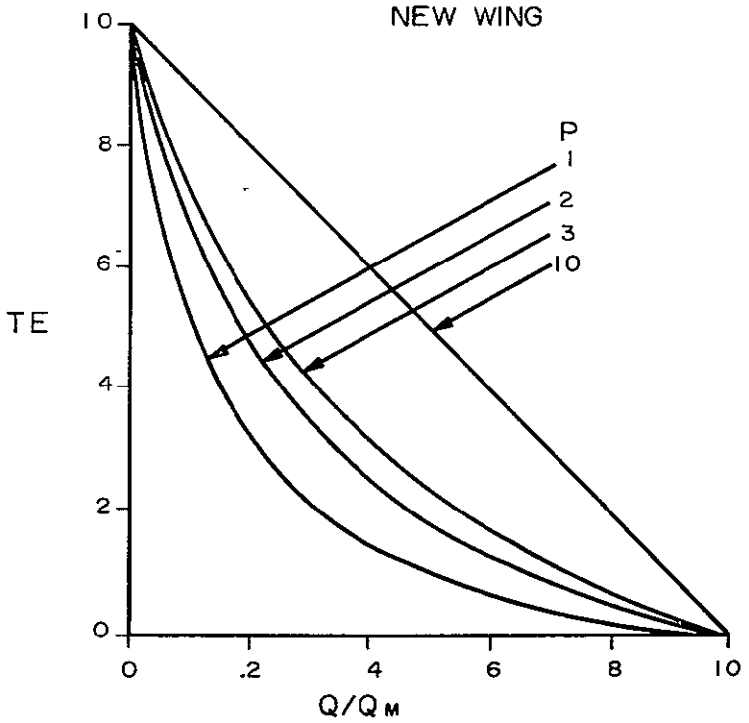

($e_t > 0$)
Fig. 24 (b)

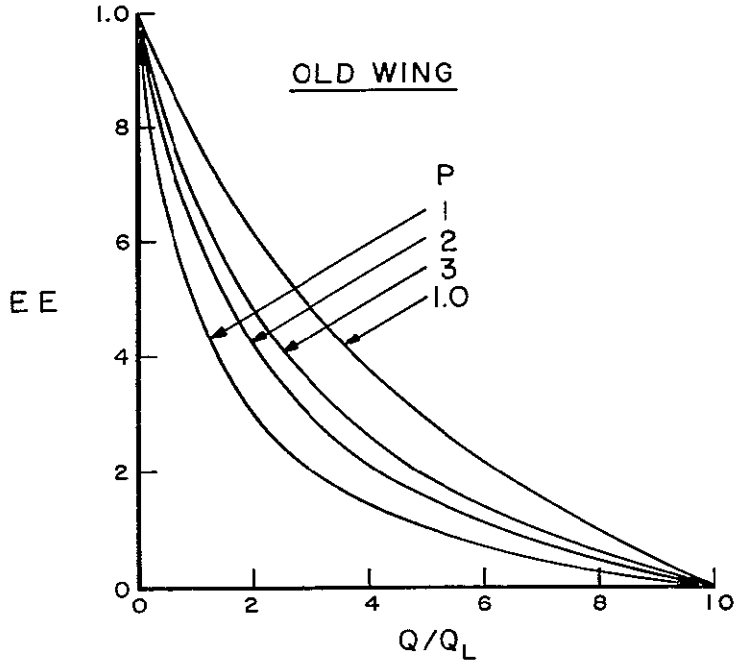

ELEVATOR EFFECTIVENESS VS Q/Q_L

($e_t < 0$)

Fig 25(a)

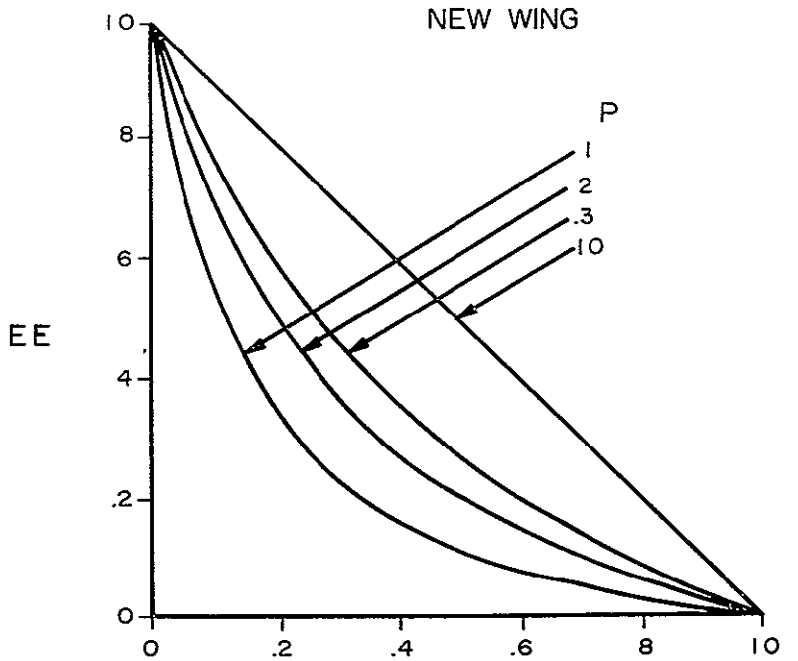

($e_t > 0$)

Fig 25(b)

Bisplinghoff et al. (1955) which include all relevant rigid body motions (plunge, pitch and roll).

Denoting the vertical displacement at x,y due to a unit vertical load at ξ,η by $C^{\delta F}(x,y;\ \xi,\eta)$, the motion dependent aerodynamic loads by $F(\xi,\eta,t,w,\dot{w},\ddot{w},\ldots)$, and the motion independent loads (such as gust loads, aircraft weight,etc.) by $F^{D}(\xi,\eta,t)$, the general equations of motion for small deformations may be written as

$$w(x,y,t) - w(0,0,t) - \frac{\partial}{\partial x}[w(0,0,t)]\ x - \frac{\partial}{\partial y}[w(0,0,t)]y =$$

$$\int_S C^{\delta F}(x,y;\ \xi,\eta)\{F(\xi,\eta,t,w,\dot{w},\ddot{w},\ldots) + F^{D}(\xi,\eta,t) - \rho(\xi,\eta)\ddot{w}(\xi,\eta,t)\}d\xi d\eta \tag{1}$$

$$\int_S \rho(\xi,\eta)\ddot{w}(\xi,\eta,t)d\xi d\eta = \int_S \{F(\xi,\eta,t,w,\dot{w},\ddot{w},\ldots) + F^{D}(\xi,\eta,t)\}d\xi d\eta \tag{2}$$

$$\int_S \rho(\xi,\eta)\ddot{w}(\xi,\eta,t)\xi d\xi d\eta = \int_S \{F(\xi,\eta,t,w,\dot{w},\ddot{w},\ldots) + F^{D}(\xi,\eta,t)\}\xi d\xi d\eta \tag{3}$$

$$\int_S \rho(\xi,\eta)\ddot{w}(\xi,\eta,t)\eta d\xi d\eta = \int_S \{F(\xi,\eta,t,w,\dot{w},\ddot{w},\ldots) + F^{D}(\xi,\eta,t)\}\eta d\xi d\eta \tag{4}$$

Equation (1) describes the elastic deformation, Eq. (2) represents force equals time rate of change of linear momentum in the vertical direction and Eqs. (3) and (4) represent moment equals time rate of change of angular momentum in the pitching and rolling angular directions, respectively.

These equations may be recognized as one variant of the dynamic response equations which are almost universally solved by the use of the truncated modal expansion schemes

and are usually not associated with the dynamic instability behavior (flutter) of the aircraft. However, by introducing the above mentioned aerodynamic and influence function representations into the set of equations [(1) through (4)] it appears possible to construct* a linear algebra (matix) flutter model that will be of the form,

$$\begin{bmatrix} \begin{bmatrix} n \times n \\ \text{Matrix} \end{bmatrix} & \begin{bmatrix} n \times 3 \\ \text{Matrix} \end{bmatrix} \\ \hline \begin{bmatrix} 3 \times n \\ \text{Matrix} \end{bmatrix} & \begin{bmatrix} 3 \times 3 \\ \text{Matrix} \end{bmatrix} \end{bmatrix} \begin{bmatrix} \{w_i\} \\ \hline w_{oo} \\ \hline \dfrac{\partial w_{oo}}{\partial x} \\ \hline \dfrac{\partial w_{oo}}{\partial y} \end{bmatrix} = \begin{bmatrix} \\ 0 \\ \\ \end{bmatrix} \leftarrow \begin{array}{c} (n + 3) \times 1 \\ \text{null column} \\ \text{matrix} \end{array}$$

where the flutter speed (eigenvalue) of the complete aircraft will be the lowest value of the speed that makes the determinant of the reduced coefficient matrix [Rank and order are different since rigid body modes are involved in the (n + 3) x (n + 3) coefficient matrix.] vanish, and the mode shape (eigenvector) will be the associated column matrix that yields all the n elastic variables as well as the three (3) rigid body generalized displacements.

This model has the capability of being developed into a "master model" for all static and dynamic problems. While

---

* The actual construction employs a weighting matrix numerical integration scheme similar to those used in lift redistribution problems [c.f. Bisplinghoff et al. (1955)].

the interim details appear laborious, the above scheme has a conceptual clarity, and it is anticipated that the final results may be used in a simple and routine manner. This will help insure that the students involved in the project have an understanding of the problem as well as an efficient computational tool.

D. Summary

The required new derivations have been completed or are in the process of being completed. They should provide the means for calculating the quantities needed to either confirm that the glider does not have aeroelastically induced deficiencies or indicate that some redesign may still be necessary.

5. Fabrication and Testing

A. Introduction

Twenty one undergraduate students are currently enrolled in the portion of the CAPGLIDE project which provides "hands on" fabrication experience in the building of the glider. Most of these students are, of course, inexperienced, and the new glider design, which has evolved since the last report, with its simplified construction scheme promises easier fabrication. (The CFRP* D-box section envisaged in the earlier design is relatively speaking, considerably more difficult to fabricate, and the associated difficulties have been circumvented by the new design.) Another bonus is that the

* Carbon fiber reinforced plastic

tapered sections of the earlier design (taken together with the cambered airfoil) would have required separate molds for each wing. The largely constant chord planform now allows one mold to be used for both wings, except for spanwise stations quite close to the wing tips.

B. Materials

To keep the weight below 100 lbs. the choice of materials is a constant challenge. During the summer a two meter mold section (of the tapered wing design) was constructed and a one meter wing section fabricated. The fabrication of this wing section was intended primarily to gain experience in lay-up techniques and to gain insights as to the problems that might be encountered. In this it was successful.

a) Resin: One problem experienced was that the resin was not completely curing. This led to an investigation of several resin and hardener systems. The resin found to have properties most suitable for our requirements was the A509 resin manufactured by Ciba Geigy. The pot and gel times for this resin, with XU224 and XU225 hardener added, is shown in Table III.

b) Glass Fabric: In the test wing section, 3-ply glass cloth was used - Burlington style 106, 0.6 ozs./yd.^{2} and .015" thick oriented at 45° to the span direction. This fabric proved very difficult to handle; it wrinkled and tore easily. Consequently, a heavier fabric (Burlington Style 112, 2.1 ozs./yd.^{2} and 0.032 mil. thick) was chosen

TABLE III
POT LIFE AND GEL TIMES FOR RESIN SYSTEM[a]

Batch	Resin (PBW)[b] A 509	Hardener (PBW) XU 224	XU 225	Pot (hr)	Gel (hr)
1	100	27	30	0.5	0.75
2	100	29	23	1.0	1.25
3[c]	100	34	15	1.5	2.5
4	100	34	9	2.5	3.5
5	100	42	0	2.5	6.0

[a] Resin System Selected

1. Manufacturer: Ciba Geigy
2. Resin: A 509 and A 508
3. Hardener: XU 224 and XU 225
   (Modified Aliphatic)
   (Amine Hardener)

[b] (PBW) parts by water

[c] Selected for layups. A 508 may be added to improve impact resistance.

for the actual wing that is to be fabricated. The wing skin is proposed to consist of a GFRP*/Polymer foam/GFPR Sandwich Structure, and this was fabricated in the trial.

c) PVC Foam: Sample coupons were made of a number of GFRP/ Polymer foam/GFRP Sandwich Systems. The foam materials tested were styrofoam, polyurethane and PVC.

Styrofoam was not suitable; apart from the fact that it is soluble in gasoline, it is also soluble in the curing agents in epoxy resins.

Polyurethane had good chemical stability, but the surface is friable and tends to separate from the GFRP skin.

PVC foam made by Klege-cell proved to have the desired properties -- low density and chemical stability. It is obtainable in sections 0.125" thick. Properties of the PVC foam are provided in Table IV.

d) Release Agent: The release agent used was not satisfactory as difficulty was experienced in separating the wing section from the mold. Subsequent trials with other release agents resulted in the choice of Miller Stephenson MS 142C which consists of particulate teflon suspended in a volatile medium.

e) Graphite Fiber: The graphite fiber to be used in the box section spars has been selected and parts fabricated in a pressure furnace. The fiber is Union Carbide T300 and is in prepreg form; -- Fiberite Hy-E 1048AE.

---

* Glass fiber reinforced plastic

TABLE IV
PROPERTIES OF TYPE 40 PVC FOAM*

1.	Average Density	2.5 lbs./ft.^{3}
2.	Thickness	0.125 inches
3.	Comp. Strength	60 psi
4.	Comp. Modulus	1750 psi
5.	Tensile Strength	75 psi
6.	Flexure Strength	90 psi
7.	Flexure Modulus	2715 psi
8.	Shear Stress	35 psi
9.	Shear Modulus	650 psi
10.	Linear Coefficient of Expansion	$2.0 - 2.2 \times 10^5$
11.	Chemical Resistance	S l. Softened by Aromatic Hydrocarbons

* Manufactured by Klege-Cell.

f) Fuselage: The fuselage of the glider will be fabricated from a Kevlar 49/balsa wood/Kevlar 49 Sandwich. This is a 3D self-supporting structure and the Kevlar/balsa sandwich is necessary to provide the required strength and rigidity.

The materials to be used in the glider are summarized in Table V.

C. Molds

a) Wing Section Mold: The wing span of the glider is 39 feet, and two molds have been constructed. These are for the upper and lower profiles of the wing. The molds are supported by wooden frames (see Schematic Figure 26). The aerodynamic profile was computer generated and transferred onto plywood templates which were spaced 2/3 meter apart. Six fiberboard ribs shaped to within 1/8" of the desired profile were spaced between the templates. These fiberboard ribs were then "ground" to the desired profile by abrading with sandpaper. This was accomplished by attaching sandpaper to a one meter rod which spanned the plywood templates and by abrading the ribs until the profile of the templates was transferred to the ribs. Sheets of countertop melamine were glued to the templates and ribs with epoxy. The melamine surface is the subsequent mold surface.

The mold surface was seen to have small undulations. These were removed by coating the surface with epoxy and silicate balloons and sanding. Finally, an acrylic paint was applied.

TABLE V
MATERIALS USED IN THE GLIDER

1. Glass Cloth

Manufacturer: Burlington

Type: Fabric Style 112
(.0032 mil. thick and
2.1 oz. $yd.^2$)

2. Graphite

Prepreg: Fiberite Hy - E 1048 AE

Cured
Properties: Ply thickness - .006"

V_f fiber - 65%

Tensile strength: 185,000 psi

Tensile modulus: 20×10^6 psi

$\nu_{21} = 0.255"$

3. Kevlar

Kevlar 49

Fig. 26

WING MOLD

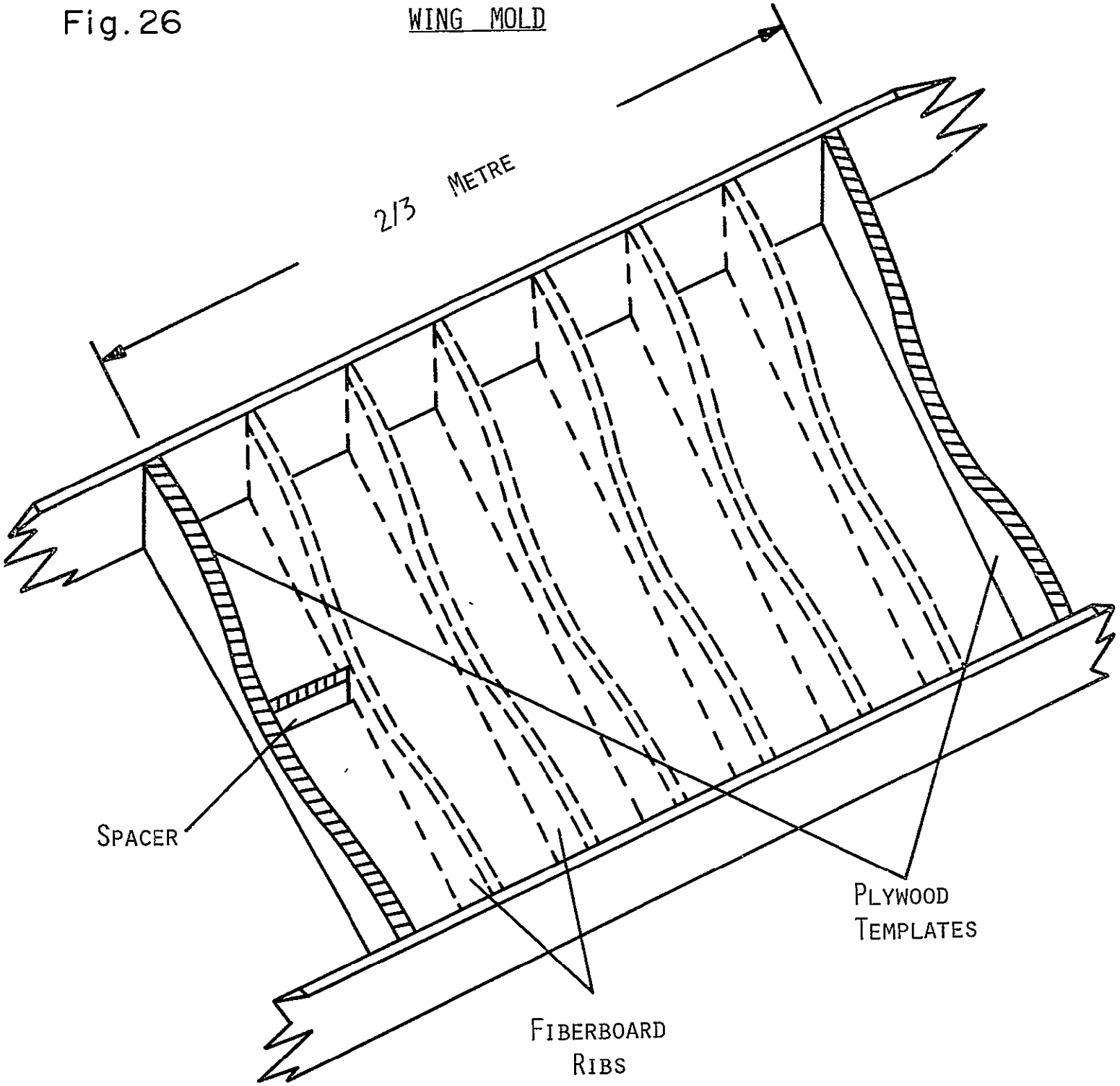

Tail-section-molds for the tail sections have been prepared in a manner similar to that for the wing section.

b) Fuselage Mold: A 3-D "male" fuselage mold is under construction, using plywood and balsa. The intention is to utilize this directly to produce the actual Kevlar/balsa/Kevlar sandwich structure.

D. Fabrication - Wing

In the trial, one meter-length-wing produced, a wet lay-up technique was used. This was successful, and the method will be used in the glider wing construction as follows:

1. Coat mold surface with release agent.
2. Brush on layer of resin.
3. Apply layer of Burlington Fabric Style 112 with fibers at ±45° to the wing axis, ensuring that the fabric is layed without wrinkles.
   NOTE: The Volume fraction (V_f) of fibers used in theoretical calculations was 40%. This V_f is considered to be the lowest value that would be achieved using this method. Care is taken to ensure that the fabric has been "completely wet" by the epoxy.
4. Apply PVC foam to "wet" glass/epoxy.
5. Vacuum bag and allow to cure (48-72 hours at room temperature).
6. Remove vacuum bag and apply resin directly to foam and lay on final glass layer.
7. Vacuum bag and repeat cure cycle.

The upper and lower wing profiles will be prepared separately. The profiles still in their molds will be mated and glued together. After curing, the skins will be "sprung" from the molds.

In the one meter test section, internal aerofoil ribs were glued into position in one of the molds before they were mated. However, these ribs are not in the final wing version and assembly has been made considerably easier.

The bending moment within the wing will be supported by a CFRP box-section spar. Similar spars will also form the booms for the glider.

E. The CFRP Box Section Spar

The "flanges" of the box section will take the bending moment and will consist of CFRP. The side walls will take the shear forces and will consist of a GFRP/foam/GFRP construction. A schematic of the cross section is shown in Figure 27.

A pressure furnace 7.5 meters long and 7.5 centimeters diameter has been built for CFRP spar production. The spars are designed to be 4.9 meters long. Standard lay-up techniques for CFRP prepreg have been used. The Fiberite HyE 1048AE prepreg was laid-up bagged, vacuum applied and heated to 79°C at a heating rate of 1.6 - 2.6°C/min. The temperature was held constant at 79°C, and pressure of 100 psi was applied. Subsequently, the temperature was raised to

Fig. 27

BOX SECTION

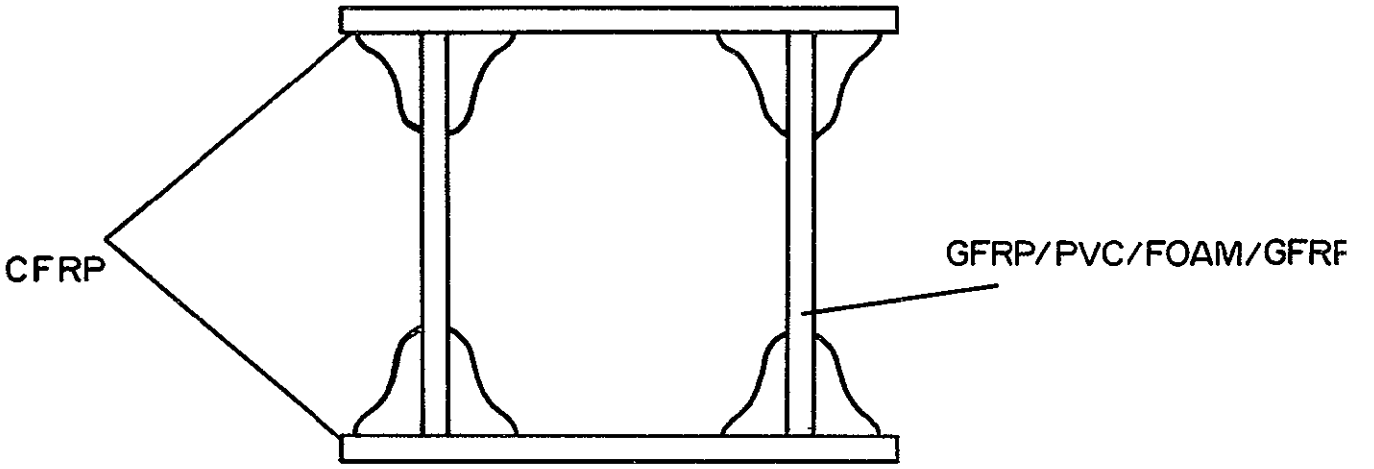

121°C at the previous heating rate and held there for two hours.

The actual spar design is shown in Figure 28 and consists of 25 plies at the root and three at the tip. All bonding surfaces are cured with a nylon peel ply to eliminate the requirement for surface preparation.

Tensile test samples were prepared using the Fiberite HyE 1048 prepreg. The results were in complete agreement with the expected values.

Fig. 28

CFRP FLANGES FOR
WING SPARS

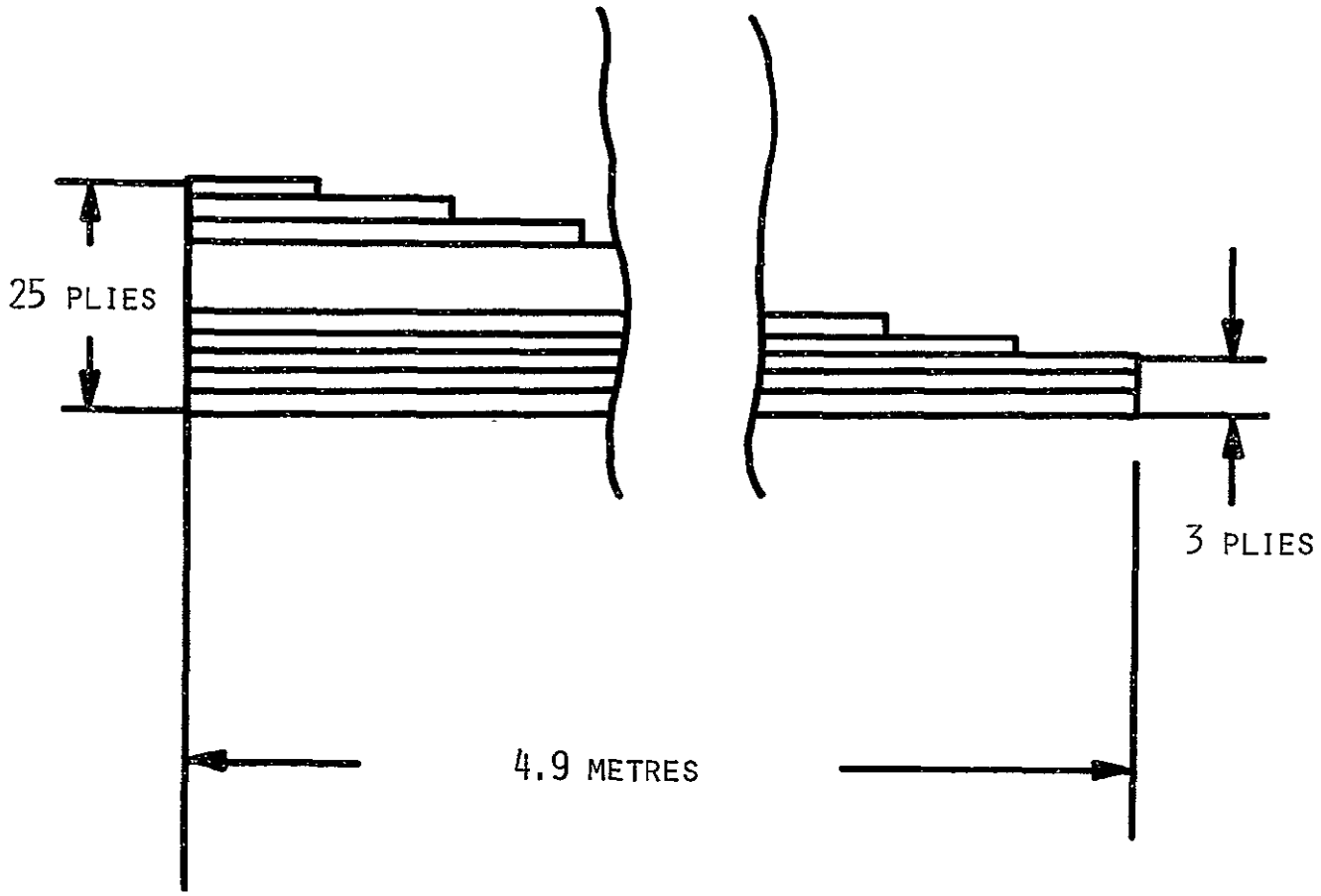

PART III

COMPAD (Computer Aided Design)

COMPAD (Computer Aided Design)
(L. J. Feeser)

The computer aided design portion of the composites project has concentrated on improvement and enhancement of the general finite element code, SPAR, on the interactive computer graphics facility within the School of Engineering at RPI.

Effort reported in previous progress reports dealt with establishing the capability of performing interactive, finite element analyses on our computer system making use of the form of the SPAR program, as initially converted by the NASA Langley group. This initial conversion of the program involved limitations imposed by the desire to run the program on a PRIME computer configuration which did not support the virtual memory operating system. As a result, the program did not take advantage of the inherently faster hardware instruction set of Rensselaer's P500 interactive graphics computer.

Efforts since April 1978 have focused on implementing the SPAR code in the virtual memory operating system environment of the P500. Run time improvements on the order of 15 to one have now been achieved. Some "clean-up" and documentation work on this phase of the implementation still remain. In addition, the simplified beginner's user manual*

---

* Barone, Thomas R. and Larry J. Feeser, "Beginner's User Manual for SPAR", Report No. 78-1, Department of Civil Engineering, Rensselaer Polytechnic Institute, Troy, N. Y., May 1978.

has been completed and is presently under review by the NASA Langley group for reprinting as a NASA report to accompany the COSMIC distribution planned for the SPAR PRIME implementation.

Work is continuing on graphics developments within the SPAR code to provide for some pre- and post-processing capability of the finite element analysis. Presently, our displays on the IMLAC interactive devices are a result of translating the device-dependent (Tektronix), undocumented graphics display code which was initially done at Langley. Two students have been familiarizing themselves with the general data structure of the SPAR program in order to develop a general pre-processor SPAR Processor which will allow communication between the PRIME IMLAC system and the SPAR data base through graphics screen interaction, which has not heretofore been possible due to the original Tektronix implementation. Some general relational data base techniques are being investigated to insure that our conversion to the IMLAC graphics has maximum portability and transference to other finite element codes. The ability to zoom and pan any interactive display of the finite element grid is under development, in addition to the rotation features already in the Tectronix implementation.

The improved graphics capability of the SPAR program will provide an excellent capability for the detailed structural analysis work to be done under the RPI composites program as described elsewhere in this report.

PART IV

SUPPORTING RESEARCH

Progress is reported in the following individual write-ups, on composites research in the following areas:

Matrix Characterization and Environmental Effects

Fatigue in Composite Structural Materials

Non-Destructive Testing

Metal Matrix Composites

Initial steps have been taken in aeroelastic research but progress is not yet sufficient to be individually reported.

RESIN MATRIX CHARACTERIZATION

Senior Investigator: S. S. Sternstein

This project emphasizes two important aspects of high performance composites research, namely (1) the viscoelastic characterization of the highly crosslinked epoxy resins and (2) the analysis and prediction of swelling stresses due to moisture absorption in epoxy resins and composites made from such resins.

1. Viscoelastic Characterization

The report period has been devoted primarily to construction and modification of a viscoelastic test apparatus to be described below and to obtaining and conditioning suitable test samples of epoxy resins. The viscoelastic tester is of the closed loop, forced oscillation type with an electromagnetic actuator. This system enables creep and relaxation (transient) tests to be performed at time scales as short as 50 milliseconds, without overshoot of the command input, either load (for creep) or displacement (for relaxation). In addition dynamic sinusoidal frequency inputs in excess of 100 Hertz can be employed to obtain dynamic storage (in-phase) and loss (out of phase) modulii.

A phase angle computer capable of resolving phase angles between stress and strain of 0.05 degrees has been acquired and permits fully automated frequency sweeps and data acquisition and reduction for sample geometry. This

instrument interfaces with a computerized temperature controller/programmer for fully automated temperature and frequency sweeps.

Two epoxy resins, Hercules 3502 and Narmco 5208, have been supplied to us in cured neat resin samples through the courtesy of General Dynamics, Fort Worth. Two specimen geometries have been fabricated, namely a circular dog-bone and a thin rectangular slab, the latter for a dynamic 3-point flexure jig. These samples are currently being conditioned at 60°C and two relative humidities, 100% and 60%, and will be ready for testing in two months. Detailed viscoelastic behavior using both transient and dynamic tests will be performed over a broad range of temperature, time scale and frequency, and humidity.

2. Inhomogeneous Swelling by Water

Previous theory by this investigator is being extended to the problem of inhomogeneous swelling by water of epoxy matrices in composites. Briefly, the problem is as follows: When a composite structure contains one phase which absorbs a diluent (e.g., water) while the second phase does not, then an inhomogeneous swelling problem exists. Such problems require simultaneous solution of the equations of stress equilibrium with the necessary thermodynamic constitutive equations. In general, large internal distributions of stress, strain and composition (i.e., water concentration) are produced by inhomogeneous swelling. We

are currently modeling the fiber-reinforced composite swelling problem on a computer graphics system. Detailed profiles of stress, strain and water distribution in the matrix will be calculated as a function of various thermodynamic parameters.

FATIGUE IN COMPOSITE STRUCTURES

Senior Investigator: E. Krempl

The literature survey continued with special emphasis on time-dependent and frequency dependent fatigue properties of composites. It was found that both time under load (hold-times) and frequency have an effect on fatigue life.

The trends of the data are similar to the trends observed in high temperature metal fatigue. Generally a decrease in frequency and an increase in hold-time decreases fatigue life.

Of particular interest are studies reporting changes in composite properties while subjected to fatigue loading; stiffness and temperature change measurements are examples.

Smooth metal specimens may cyclically harden or soften. As a consequence the residual strength of metals may increase or decrease relative to the virgin strength. We have not found a report, however, showing cyclic hardening of smooth composite specimens. All the data show softening and a corresponding decrease in residual strength (the reported increase of the residual strength of notched specimens is not due to an intrinsic residual strength increase of the material; it is rather caused by a blunting of the notch due to progressive damage).

We intend to monitor progressive changes in our composite specimens during fatigue loading, with primary emphasis on temperature.

In a first attempt to generate fatigue data we decided to investigate the uniaxial properties of unidirectional laminates. We have made 12-ply unidirectional laminates out of NARMCO Rigidite 5208 carbon fiber prepreg system (the material was donated by NARMCO) using the cure cycle recommended by the manufacturer.

Two types of specimens were designed, each with tabs at the end. The first specimen is rectangular, .5" (1.27 cm.) wide and 4-3/4" (12.07 cm.) long. The second specimen has the same length but is bow-shaped with a .5" (1.27 cm) minimum width. We will test eight specimens of each design to see which has the best fatigue performance. Uniaxial tests will be used as base line data for future biaxial tests.

ULTRASONIC NON-DESTRUCTIVE TESTING OF COMPOSITE STRUCTURES

Senior Investigators: H. F. Tiersten
P. K. Das

During the reporting period the experimental difficulty encountered in measuring the influence of a tuning inductor on the bandwidth and sensitivity of the trapped energy mode transducer for relatively large values of inductance has been overcome. The results that have been obtained are in excellent agreement with the theoretical predictions. Tuning inductors are now being employed routinely to increase both the sensitivity and bandwidth of the monolithic mosaic transducer utilizing trapped energy modes. Since the inductance will be set to optimize sensitivity at mid-band, further increases in bandwidth will be obtained by mechanical means. Recent experiments with the tuned, trapped energy mode mosaic transducer seem to indicate that the sensitivity is greater than that obtained with any of the commercially available transducers we have obtained to date. An imaging capability has recently been established in the Microwave Acoustics Laboratory and some good images of simple objects have been obtained.

The velocities of acoustic surface waves in a number of composite materials have been measured. Since some difficulties have been encountered in using the recently developed electromagnetic and electrostatic non-contact transducers for the excitation of surface waves in non-conducting

composite materials, a wedge transducer, which requires contact, has been used. It has been found that the wedge transducer does not simply excite a surface wave but rather excites the fundamental extensional (symmetric) and flexural (antisymmetric) plate waves, which are the only ones possible in the composite plate because it has two major surfaces. In the frequency range employed, both waves have velocities very near that of the surface wave, but differing slightly. At the lateral position of excitation on the upper surface the effect of the two waves nearly cancels at the lower surface and reinforces at the upper one so that nearly all the energy appears as a surface wave at the upper surface. However, because of the slight difference in velocity of the two waves, at some distance downfield from the point of excitation of the surface wave, all the energy appears to be concentrated as a surface wave at the lower surface. An additional traversal of that distance results in the appearance of the surface wave at the upper surface and so on. The coupling length varies with frequency in accordance with the dispersion curves for the fundamental extensional and flexural waves in the composite plate.

An analysis of a fully electroded thickness-extensional vibrator with a tuning inductor in the driving circuit has been performed, and the influence of a tuning inductor on the resonant frequency of thickness vibration has been calculated; as noted above, the agreement with experiment is

excellent. The dispersion curves for the pertinent fundamental extensional waves in an infinite PZT-7A plate have been obtained from the appropriate two-dimensional solutions for both the unelectroded case and that of shorted electrodes. The calculation shows that the bandwidth of the PZT-7A thickness-extensional trapped energy mode transducer must be less than 25%. Combinations of the solutions for the infinite plate have been employed in an appropriate variational principle of linear piezoelectricity to obtain a very accurate approximate two-dimensional solution for the trapped energy eigenmodes in the partially electroded, unloaded PZT-7A plate. The resulting frequency spectra for the first few trapped energy modes have been obtained. This latter information can be employed to decide on trade-offs dictated by systems requirements in order to determine the optimum width of the electrodes for a particular linear phased array imaging system.

METAL MATRIX COMPOSITES

Senior Investigator: N. S. Stoloff

The objective of this project is to utilize microstructural control to optimize mechanical behavior of eutectic composites. Previous investigations of mechanical properties of aligned eutectics generally have been concerned with alloys consisting of brittle fibers and ductile matrices. The Ni-Al-Mo system is unusual in that at room temperature it consists of a ductile γ/γ' matrix (the relative amounts of each phase depending upon Al content) and ductile Mo (α) fibers. The eutectic reaction at the melting temperature is between γ and α.

Tension and compression tests previously have been performed in the range 25°C to 800°C on two aligned pseudo-eutectic alloys: AG15 (Ni-17.7a/oAl-16.3a/oMo) and AG34 (Ni-14.4a/oAl-20.0a/oMo). The yield stress in tension for both alloys was greater than in compression at all test temperatures. Anisotropy of yielding was shown to arise from a difference in deformation mechanisms in tension and compression, rather than to residual stresses arising from different thermal expansion coefficients of the co-existing phases.

Ultimate tensile strength decreased while yield strength increased with temperature to 800°C for both alloys. Compressive 0.2% yield strength increased with

temperature to 600°C and then decreased at 800°C. At 800°C, necking of the tensile specimen occurs as a result of ductile failure of fibers and matrix, while a compression specimen with 6% total strain was found to exhibit in-phase fiber buckling and fiber shear. No such deformation was found at 25°C.

During the present report period transmission microscopy and electron diffraction experiments on a solutionized AG34 sample have confirmed the orientation relationship between γ and α to be: $(100)_\gamma \parallel (110)_\alpha$. Both phases grow parallel to <001>.

Room temperature fatigue testing of Ni-Al-Mo alloys in the as-D.S. condition revealed behavior characteristics of other fibrous eutectics. Further progress has been made in our program of elevated temperature fatigue testing. The fatigue life of AG34 (0.76 cm/hr) exceeds that of AG15 (1.9 cm/hr) at room temperature. This superiority in fatigue response is also evident in testing performed at 825°C and in a vacuum of 10^{-6} torr.

Scanning electron microscopy (SEM) was used to compare fatigue fracture surfaces of specimens tested at the two temperatures. Surface crack initiation occurred at room temperature; however, internal nucleation was evident at 825°C. Since some creep-fatigue interaction is likely to account for the latter observation, SEM fractography comparisons on both fatigue and creep fracture surfaces are

necessary. To further clarify the mode of fracture, fatigue test frequencies of 0.2, 20 and 50 Hz will be used in high temperature tests on AG15.

As part of a general program to determine whether internally charged hydrogen embrittles nickel-base eutectics, several delayed failure experiments have been run on notched tensile samples of AG34. Samples that were pre-charged with hydrogen and then tested revealed a small difference in properties relative to uncharged samples. However, simultaneous charging and testing revealed a considerably higher susceptibility of this alloy to the presence of hydrogen.

We have previously shown that the Ni-Al-Mo system is subject to significant γ' (Ni_3Al) precipitation hardening. AG34 specimens will be solutionized at 1260°C for 4 hours and aged at 850°C for 1 hour. Fatigue properties in the heat-treated and as-D.S. conditions will be compared in tests performed at room temperature and under high vacuum conditions.

In addtion, fatigue crack propagation (da/dN) experiments will be performed on AG34. Extensive transmission electron microscopy will be employed to characterize dislocation substructure and precipitate-dislocation interactions.

PERSONNEL

Senior Investigators

Brunelle, E. J., Jr., Sc.D. (Aeroelastic and structures design and analysis, CAPGLIDE)*	Associate Professor of Aeronautical Engineering
Das, P. K., Ph.D. (Non-destructive evaluation, research)*	Professor of Electrical and Systems Engineering
Diefendorf, R. J., Ph.D. (Fabrication, CAPGLIDE; fiber behavior, research)*	Professor of Materials Engineering
Feeser, L. J., Ph.D. (Computer applications and graphics, computer aided design, optimization)*	Professor of Civil Engineering
Hagerup, H. J., Ph.D. (Aerodynamics, configuration, pilot accommodation, CAPGLIDE)*	Associate Professor of Aeronautical Engineering
Helwig, G., Dr.Ing. (Finite element methods, computer aided design, composite structure optimization, CAPGLIDE)*	NASA/AFOSR Visiting Research Associate
Hirano, Y., Ph.D. (Structures, composite buckling)*	Visiting Professor of Aeronautical and Mechanical Engineering
Hoff, N. J., Ph.D. (Structural design and analysis, CAPGLIDE)*	John A. Clark and Edward T. Crossan Professor of Engineering
Krempl, E., Dr.Ing. (Fatigue studies, research)*	Professor of Mechanics and Director of Cyclic Strain Laboratory
Sternstein, S.S., Ph.D. (Failure analysis, matrix behavior, research)*	William Weightman Walker Professor of Polymer Engineering

* Fields of Speciality

Stoloff, N. S., Ph.D. (Directionally solidified eutectics, research)*	Professor of Materials Engineering
Tiersten, H. F., Ph.D. (Non-destructive evaluation theory, research)*	Professor of Mechanics

Research Staff

Research Associates

Kenmochi, Kiyoshi, Ph.D.
Sinha, Bikash K., Ph.D.

Graduate Assistants

Barone, Thomas, B.S.
Brundage, Barbara A., B.S.
Chan, Ka-Tung, B.S.
Chen, Lien-Wen, M.S.
Crane, Carl, B.S.
Ely, Dale R., B.A.
Hess, Jeffrey W., B.S.
Hongo, Sho-ichi, B.S.
Hoskote, Mangesh, B.E.
Kim, Wonsub, B.S.
Klein, Leigh, B.S.
Lanzl, Colon, B.S.
Messian, Javid, B.S.
Muser, Cristoph, Dipl.Mech.Ing.
Robinson, A., B.S.
Rosenthal, Jay, B.S.
Shick, D. V., B.S.
Sundaram, Viswanath, M.S.
Talley, S., B.S.
Tartaglia, John M., B.S.
Teferra, Michael, M.S.
Van Shoonveld, H. Garrit, B.S.
Yang, Phillip, B.S.

Undergraduate Assistants - Seniors**

Berg, R. William
Conway, Christopher
Fedor, Michael J.
Fisher, Mark Thomas
Heath, Jeffrey A.
Jaran, Chris
Koopersmith, David M.
Loeffler, William J.
McDevitt, Mark R.
Morano, Joseph S.
Parlini, Francis E.
Perron, David E.

---

* Fields of Speciality
** Status prior to Commencement and end of term in the Spring of 1978.

Undergraduate Assistants - Seniors (contd.)**

Tortorici, Mark	Weiner, Steven D.
Villaneuva, Humberto	Zmroczek, Leon A.

Undergraduate Assistants - Juniors **

Abranovic, Paul M.	Munro, Thomas E.
Antonier, Eugene, B.S.	O'Neil, Patrick
Chisholm, Brian C.	Reusch, David
Donnelly, J. Patrick	Schwager, Bruce H.
Ezzo, Jeffrey	Shaefer, Paul
Goldstein, Kevin	Shoales, Gregory A.
Hoffert, William D.	Speicher, Terrance L.
Kearns, Thomas	Sutton, Jeffrey A.
Lenyo, John S.	Weisenger, Norman
Melnyk, Michael S.	Zeman, Raymond

Undergraduate Assistants - Sophomores **

Coy, Paul F.	Rodgers, R. George
Martone, Stephen M.	Zelenski, Warren E.

** Status prior to Commencement and end of term in the Spring of 1978.

AUTHOR INDEX

	Page
Brunelle, E. J., Jr.	18
Das, P. K.	73
Diefendorf, R. J.	18
Feeser, L. J.	65
Hagerup, H. J.	18
Helwig, G.	18
Hirano, Y.	11
Hoff, N. J.	11,18
Krempl, E.	71
Sternstein, S. S.	68
Stoloff, N. S.	76
Tiersten, H. F.	73